SGIP1 modulates kinetics and interactions of the cannabinoid receptor 1 and G protein-coupled receptor kinase 3 signalosome

Matej Gazdarica, Judith Noda, Oleh Durydivka, Vendula Novosadova, Ken Mackie, Jean-Philippe Pin, Laurent Prézeau, Jaroslav Blahos

SGIP1 modulates kinetics and interactions of the cannabinoid receptor 1 and G protein-coupled receptor kinase 3 signalosome

Matej Gazdarica[1, 2], Judith Noda[1], Oleh Durydivka[1], Vendula Novosadova[3], Ken Mackie[4], Jean-Philippe Pin[2], Laurent Prezeau[2, 5], Jaroslav Blahos[1, 5]

[1] *Institute of Molecular Genetics, Czech Academy of Science, Videnska 1083, 14220 Prague 4, Czech Republic*

[2] *Institut de Génomique Fonctionnelle, Université Montpellier 1 and 2, Montpellier, France*

[3] *The Czech Center for Phenogenomics, Institute of Molecular Genetics of the Czech Academy of Sciences, Prumyslova 595, 252 50 Vestec, Czech Republic*

[4] *Department of Psychological and Brain Sciences, Gill Center for Molecular Bioscience, Indiana University, 1101 E. 10th St., Bloomington IN USA, 47405*

[5] *These authors contributed equally*

Corresponding author: Jaroslav Blahos, jaroslav.blahos@img.cas.cz

Abbreviations list

AP-2 - Adaptor Protein 2

BRET - Bioluminescence energy transfer

CB1R - Cannabinoid receptor 1

Cat. no. - catalogue number

CME - Clathrin-mediated endocytosis

CNS - Central nervous system

DMEM - Dulbecco's Modified Eagle Medium

ECS - Endocannabinoid system

FBS - Fetal bovine serum

FCHo - FCH/F-BAR domain only protein

GPCR - G protein-coupled receptor

GRK - G protein-coupled receptor kinase

HEK293 - Human embryonic kidney 293

mBRET - miliBRET

PBS - Phosphate-buffered saline

PBST - Phosphate-buffered saline solution with Tween

PH - Pleckstrin Homology

RH - Regulator of G protein signaling Homology

Rluc - *Renilla* luciferase

RRID - Research Resource Identifier (see scicrunch.org)

SGIP1 - Src homology 3-domain growth factor receptor-bound 2-like 1

SR141716 -rimonabant

YFP - Yellow fluorescent protein

WIN - WIN 55,212-2 mesylate - [(3R)-2,3-dihydro-5-methyl-3-(4-morpholinylmethyl)pyrrolo[1,2,3-de]-1,4-benzoxazin-6-yl]-1-naphthalenyl-methanone, monomethanesulfonate;

βarr - β-arrestin

Abstract

Cannabinoid receptor 1 (CB1R), a G protein-coupled receptor, plays a fundamental role in synaptic plasticity. Abnormal activity and deregulation of CB1R signaling result in a broad spectrum of pathological conditions. CB1R signaling is regulated by receptor desensitization including phosphorylation of residues within the intracellular C terminus by G protein-coupled receptor kinases (GRKs) followed by endocytosis. Furthermore, CB1R signaling is regulated by the protein Src homology 3-domain growth factor receptor-bound 2-like (SGIP1) that hinders receptor internalization, while enhancing CB1R association with β-arrestin.

It has been postulated that phosphorylation of two clusters of serine/threonine residues, ^{456}SMGDS^{429} and ^{460}TMSVSTDTS^{468}, within the CB1R C-tail controls the association dynamics of the receptor with interaction partners involved in desensitization. Several molecular determinants of these events are still not well understood. We hypothesized that the dynamics of these interactions are modulated by SGIP1.

Using a panel of CB1Rs mutated in the aforementioned serine and threonine residues, together with an array of Bioluminescence energy transfer-based (BRET) sensors , we discovered that GRK3 forms complexes with Gβγ subunits of G proteins that is largely independent from its interaction with CB1R. Furthermore, CB1R interacts only with activated GRK3, and the dynamics of this interaction depend on the presence of specific serine and threonine residues. Interestingly, phosphorylation of two specific residues on CB1R triggers GRK3 dissociation from the desensitized receptor. SGIP1 increases the association of GRK3 with Gβγ subunits of G proteins, and with CB1R. Altogether, these data suggest that the CB1R signalosome complex is dynamically controlled by sequential phosphorylation of the receptor C-tail, and is modified by SGIP1.

Keywords

G protein-coupled receptors; Cannabinoid receptor 1; G protein-coupled receptor kinase; β-arrestin, phosphorylation, SGIP1

Highlights

Activation of GRK3 is required for its interaction with CB1R

Termination of CB1R-GRK3 interaction is regulated by phosphorylation of specific CB1R residues.

Recruitment of GRK3 and β-arrestin2 to CB1R is dependent on distinct phosphorylation patterns

SGIP1 profoundly modifies the dynamics of signalosome interactions during CB1R desensitization.

Introduction

Cannabinoid receptors, together with their endogenous ligands, endocannabinoids, and the enzymes responsible for their synthesis and degradation, constitute the endocannabinoid system (ECS). Cannabinoid receptor 1 (CB1R), a member of the G protein-coupled receptor (GPCR) family, is a central molecule of the ECS. In the CNS (central nervous system), CB1R is principally located presynaptically on many GABAergic, glutamatergic, cholinergic, serotonergic and noradrenergic neurons. CB1R is involved in fine-tuning of synaptic transmission. Activation of the CB1R suppresses neurotransmitter release in these synapses (Marsicano & Lutz 1999; Haring *et al.* 2007; Kirilly *et al.* 2013). It is expressed in circuits important for the processing of anxiety, fear, stress, motor, cognitive and social functions, including the basal ganglia, hippocampus, prefrontal cortex, amygdala and cerebellum (Herkenham *et al.* 1990; Katona & Freund 2012). ECS malfunction is linked to numerous pathological states of the nervous system (Pacher & Kunos 2013; Araque *et al.* 2017).

Chronic activation of CB1R leads to tolerance. Understanding the mechanisms leading to the development of tolerance is central for rational pharmacological management of disease states in which the endocannabinoid system is involved. The activity of the receptor is tightly regulated. Upon stimulation, CB1R follows the desensitization process common for most GPCRs that typically result in phosphorylation, uncoupling from G protein, and endocytosis of the receptor, and subsequent degradation, or recycling of receptors back to plasma membrane (Cahill *et al.* 2017; Leterrier *et al.* 2004; Fletcher-Jones *et al.* 2020). Intriguingly, different from other GPCRs, CB1R internalization is tightly controlled by interaction with the protein Src homology 3-domain growth factor receptor-bound 2-like endophilin interacting protein 1 (SGIP1) (Hajkova *et al.* 2016). SGIP1 associates with the CB1R in presynaptic elements of neurons and hinders endocytosis of the activated CB1Rs, which leads to a prolonged association between the desensitized CB1R and β-arrestin2 (Hajkova *et al.* 2016).

Stimulation of CB1R triggers several signaling pathways, including GRK activation (Jin *et al.* 1999; Nogueras-Ortiz & Yudowski 2016) that mediate phosphorylation of serine/threonine residues of the CB1R C-termini, leading to β-arrestins recruitment (Moore *et al.* 2007; Garcia *et al.* 1998; Al-Zoubi *et al.* 2019).

GRKs are serine/threonine protein kinases with a common modular structure consisting of a catalytic domain within a Regulator of G protein signaling homology (RH) domain that is flanked by N-terminal α-helical domain (αN-helix) and a variable C-terminal lipid-binding region. GRKs are soluble proteins that utilize distinct mechanisms to bring them to the close proximity of membrane-embedded GPCRs. Unlike other families of GRKs that localize to the membrane via palmitoylation (GRK1/7) or prenylation (GRK4/5/6) of C-termini, GRK2/3 use unique pleckstrin homology (PH) domain to bring this kinases to the vicinity of GPCRs (Gurevich *et al.* 2012; Koch *et al.* 1993). Upon activation of G proteins by GPCR, GRK2/3 interact with Gβγ via PH domain, recruiting kinases to the membrane and proximity of the activated receptor. This process seems to contribute to allosteric activation of the receptor-phosphorylation activity of GRK2/3, as disruption of interaction of GRK2 with Gβγ results in inhibition of GRK2-driven receptor phosphorylation (Carman *et al.* 2000; Lodowski *et al.* 2005; Pitcher *et al.* 1992).

Two regions within the CB1R C-tail contain clusters of serine and threonine residues that are phosphorylated (Hsieh *et al.* 1999; Jin *et al.* 1999; Daigle *et al.* 2008b; Morgan *et al.* 2014; Straiker *et al.* 2012; Blume *et al.* 2017; Singh *et al.* 2011; Bakshi *et al.* 2007). One motif is between residues 456 and 429, namely ^{456}SMGDS^{429} and another is between residues 460 and 468, ^{460}TMSVSTDTS^{468}. The precise roles of each of these two regions are still not clear. β-arrestins association with the

receptor mediates interaction with the Adaptor protein 2 (AP-2) complex, leading to clathrin-mediated receptor internalization. SGIP1 interacts with CB1R C-terminal domain and hinders its internalization. In this study, we investigated the dynamics of the association between GRK3 and CB1R and the role of phosphorylation of residues within both the ^{456}SMGDS^{429} and ^{460}TMSVSTDTS^{468} motifs using an alanine scanning approach together with complementary bioluminescence resonance energy transfer-based (BRET) sensors.

While β-arrestin2 binding to the activated CB1R is dependent on GRK2/3 activity that phosphorylates the CB1R C-tail in both motifs, GRK3 binding is differentially controlled by both phosphorylated motifs. In the presence of SGIP1, internalization of CB1R is hindered, with profound functional and behavioral consequences (Dvorakova *et al.* 2021; Hajkova *et al.* 2016). Characterization of interactions involved in CB1R desensitization represents an important step in understanding all phases of cannabinoid signaling.

Methods

The experiments in this manuscript are not pre-registered and no blinding procedure was performed in this manuscript. No statistical method is employed to predetermine the sample size of the experiments. No randomization methods were used.

Chemicals

Reagents for cell culture and transfection were purchased from Thermo Fisher Scientific Inc. (USA). CB1R agonist WIN 55,212-2 mesylate (WIN) was obtained from Tocris R&D, USA (cat. no. 1038) and GRK2/3 inhibitor cmpd101 was purchased from Hello Bio Ltd., UK (cat. no. HB2840).

Expression vectors and mutagenesis

Expression vectors for SGIP1-Flag, β-arrestin2-Rluc, $G\alpha_{i1}$-Rluc8, $G\beta_2$-Flag, Gγ2-YFP (Gβγ in the following text), and empty vector pRK6 used in this study have been described previously (Hajkova *et al.* 2016; Brule *et al.* 2014; Charest & Bouvier 2003). SGIP1-mCherry was constructed in house. Fragment containing full coding sequence of SGIP1 (Hajkova *et al.* 2016) was inserted into a prk5_mCherry using BamHI/SalI restriction sites creating SGIP1 fused with N-terminal mCherry tag. The CB1R mutant variants were produced either by PCR mutagenesis using QuikChange II Site-directed mutagenesis kit (Agilent, USA, cat. no. 200524) following the manufacturer's instructions using modified primers (Liu & Naismith 2008) or by replacing C-tail sequence of full-length human CB1R by synthetized CB1R C-tail DNA fragments (GeneCust, France). Plasmid coding full-length CB1R S456A, S429A that served as a template for mutagenesis was from the laboratory of Ken Mackie from Indiana University, Bloomington, Indiana, USA (Jin *et al.* 1999). Newly synthesized mutant CB1Rs variants were fused with either YFP (C-terminal) or SNAP-Tag (N-terminal). Synthetic RLuc8 coding sequence (Addgene, France, cat. no. 87121) was cloned in-frame downstream of the human GRK3 coding sequence and a triple glycine residues linker was included between the tag and GRK3 sequence and subcloned into pcDNA3. All constructs were sequenced prior their use. All plasmids were propagated in *E. Coli DH5α* (NEB, USA, cat. no. C2987H). The plasmids were purified using Qiagen Midiprep kits (Qiagen, Germany, cat. no. 12123).

Cell culture and transfections

Human embryonic kidney 293 (HEK293, RRID:CVCL_0063) cells were grown in Dulbecco's Modified Eagle Medium (DMEM) (Thermo Fisher Scientific, USA, cat. no. 21969035) containing 10 % fetal bovine serum (FBS) and maintained at 37 °C, 95 % humidity and 5 % CO_2. 24 hours before the experiment, 150 ng DNA/well was used to transiently transfect $5x10^4$ cells/well in 96-well plates (Merck, Germany, cat. no. M0187-32EA) coated with poly-L-ornithine (Merck, Germany, cat. no. P4957) using Lipofectamine™ 2000 (Thermo Fisher Scientific, USA, cat. no. 11668019) according to the manufacturer's instructions. HEK293 cell line was used up to 30th passage. The cells used in this manuscript are not listed as a commonly misidentified cell line by the International Cell Line Authentication Committee. No authentification has been conducted during the experiments.

Imaging

Cells were seeded onto culture dishes for microscopy and transfected by correspondent plasmids. Live cells were imaged at 37°C using inverted fluorescent microscope Leica DMI6000 with confocal extension Leica TCS SP5 AOBS TANDEM confocal superfast scanner, objective 63 x 1.4 oil (Leica Microsystems, Germany). Samples were excited with argon laser 514 nm and detected with a HyD detector in the range 535 - 545 nm. Microscopic images were processed in ImageJ.

Bioluminescence resonance energy transfer assays

To assess the association dynamics between studied molecules, Bioluminescence resonance energy transfer (BRET) assay was used (Xu *et al.* 1999). First, cells were seeded and transiently transfected as described in Cell culture and transfections. 24 hours after transfection, cells were washed with PBS and coelenterazine h (NanoLight, USA, cat. no. CAT#301) was added to a final concentration 5 µM. The stimulation of the cells by ligand and the BRET signal reading was performed 5 min after exposing cells to coelenterazine h using Mithras LB 940 microplate reader (Berthold Technologies, Germany) equipped with donor (480 ± 20 nm) and acceptor (540 ± 40 nm) filters. The BRET signal ratio was calculated as the emission of the energy acceptor molecules (540 ± 40 nm) divided by the emission of the energy donor molecules (480 ± 20 nm). The data are presented as the agonist-promoted mBRET (miliBRET) change that was calculated by subtracting the BRET ratio obtained in the absence of agonist from the one obtained following agonist application and multiplied by 1000 (Suppl. Fig. 1E).

Immunoblot analysis

Expression levels of CB1R-YFP mutant variants were assessed using western blot analysis. Briefly, HEK293 cells transfected with a particular CB1R-YFP variant or empty plasmid pRK6 (mock) were washed with ice-cold PBS and harvested in PBS complemented with cOmplete™ EDTA-free Protease Inhibitor Cocktail tablet (Merck, Germany, cat. no. 4693132001) followed by centrifugation 13,000x g for 10 minutes at 4°C. Supernatants were aspirated and the pellets were resuspended in PBS with protease inhibitor. Afterward, the cells were disrupted by ultrasonication (IKA, Germany) and the total amount of protein in each lysate was determined using Bradford Reagent-based assay (Sigma-Aldrich, Czech Republic, cat. no. B6916-500ML) following the manufacturer's instructions. The samples were then treated in SDS-PAGE treatment buffer (0.25 M Tris-Cl, 8 % SDS, 20 % glycerol, 0.02 % bromophenol blue, 0.04 M DTT, pH 6.8) for 10 minutes at 85°C.

Lysates were separated by 10 % SDS polyacrylamide gel electrophoresis. Subsequently, the proteins were transferred to nitrocellulose membrane (Pall Corporation, USA, cat. no. 66485) and the membrane was blocked in 5 % blotting-grade powdered milk (Carl Roth, Germany, cat. no. 68514-61-4) in PBST buffer. Afterward, the membrane was cut into two pieces and labeled either with primary antibody mouse anti-GFP (1:400, Roche, CH, Cat#11814460001) followed by secondary antibody labeling goat anti-mouse IgG-HRP antibody (1:10,000, Promega, USA, Cat#W4021) for detection of CB1R-YFP variants or with primary antibody rabbit anti-actin (1:500, Sigma-Aldrich, Czech Republic, Cat#SAB4291137) followed by secondary goat anti-rabbit IgG-HRP antibody (1:10,000, Promega, USA, Cat#W4018) for the detection of actin to check the equal loading and protein transfer.

The proteins of interest were visualized by chemiluminescence using the SuperSignal West PICO chemiluminescent substrate (Thermo Fisher Scientific, USA, cat. no. 34579) and detected on the LAS-300 system (Fujifilm, USA).

Statistical analysis

Unless stated otherwise, data represent the mean ± SEM of at least three expriments of independent cell preparations performed in triplicates. Sample sizes used for the study were determined based on previous studies of a similar nature (Hajkova *et al.* 2016). The data were not assessed for normality and no test for outliers was conducted. Statistical analysis was performed using two-way ANOVA followed by Sidak's multiple comparisons test using GraphPad Prism 7 (GraphPad Software, Inc, USA).

Ethical statement

Ethical approval was not required for this study.

Results

Site-directed mutagenesis within CB1R C-tail

To study the role of GRK2/3 in CB1R regulation we mutated serines and threonines within the ^{456}SMGDS^{429} and ^{460}TMSVSTDTS^{468} motifs. We mutated serine and threonine residues either into alanine residues that do not undergo phosphorylation or into negatively charged aspartic acids residues that partially mimic a phosphorylated state **(Fig. 1A)**. We verified the levels of expression of WT and mutated CB1R forms by immunoblotting **(Suppl. Fig. 2E)**. The multiple bands detected in western blot do not appear in a sample derived from the cells transfected with empty vector (mock), and likely represent distinct CB1R forms such as receptor dimers and /or post-translationally modified receptors (glycosylation etc.) (Wager-Miller *et al.* 2002; de Jesus *et al.* 2006). Proper cellular localization of the proteins was analyzed by confocal fluorescent microscopy **(Fig. 1B)**. All mutant receptors were functional, as monitored using the BRET-based $G\alpha_{i1}$-Gβγ protein activity sensors **(Suppl. Fig. 1D & Suppl. Fig. 2B - D).** Activation of mutated CB1R by WIN55,212-2 (WIN) (1 μM) in transiently transfected HEK293 cells induced a decrease of the BRET signal resulting from the dissociation/conformational change of $G\alpha_{i1}$-Rluc8/Gγ-YFP complex. Prior to adding the agonist, the BRET signal remained stable and then declined upon WIN application over 10 minutes **(Suppl. Fig. 2B & C**). This establishes that the CB1R C-tail phosphorylation mutants retain the ability to activate $G\alpha_{i1}$ protein signaling pathway. Moreover, the extent and potency of this activation of G proteins was similar in all tested CB1R mutants ($logEC_{50}$ for $G\alpha_{i1}$ activation; CB1R = -7.169; CB1R_2A = -7.128; CB1R_6A = -7.007; CB1R_8A = -7.146) **(Suppl. Fig. 2D)**. Thus, an inability to phosphorylate various residues within CB1R C-tail regions ^{456}SMGDS^{429} and ^{460}TMSVSTDTS^{468} does not affect acute $G\alpha_{i1}$ protein activation.

Activation of GRK3 is necessary for its optimal association with Gβγ

During GPCR mediated signaling, Gβγ subunits may interact with GRK3. In HEK293 cells co-expressing CB1R, GRK3-Rluc8 and Gβγ-YFP **(Suppl. Fig. 1D)**, WIN-induced activation of CB1R resulted in a rapid GRK3-Rluc8-Gβγ-YFP association, as shown by the increase of BRET signal **(Fig. 2A)**. In this experiment, the GRK2/3 inhibitor cmpd101 significantly reduced the interaction between GRK3-Rluc8 and Gβγ-YFP, upon WIN stimulation (mBRET values ± SEM in 15 minutes: CB1R = 161 ± 7.34; CB1R + cmpd101 = 49.1 ± 3.24).

Therefore, GRK3 in its active state is required for optimal association with Gβγ.

Blocking GRK3 catalytic activity obliterates its interaction with CB1R

Next, we studied whether the activity of GRK3 is required for its recruitment to CB1R. In HEK293 cells, we transiently expressed CB1R-YFP and GRK3-RLuc8 to monitor their association using BRET signal analysis **(Suppl. Fig. 1 A)**. Application of the CB1R agonist WIN induced a rapid increase in BRET efficiency, consistent with the formation of CB1R-GRK3 complexes **(Fig. 2B)**. This was completely suppressed by pretreatment with the CB1R selective inverse agonist rimonabant (SR141716), while WIN application had no effect on the BRET signals in HEK293 cells transfected with the metabotropic glutamate receptor mGluR1a **(Suppl. Fig. 2A)**. The GRK2/3 inhibitor cmpd101 binds to the GRK2/3 active site and renders the kinase catalytically inactive (Thal *et al.* 2011; Ikeda S 2007). This GRK2/3 activity blocker almost completely suppressed the agonist-driven increase in BRET signal between CB1R-YFP and the GRK3-RLuc8 (mBRET values ± SEM in 5 minutes: CB1R =

22.45 ± 1.57; CB1R + cmpd101 = 3.88 ± 1.73) **(Fig. 2B)**. Thus, GRK3 catalytic activity is required for its association with the activated CB1R.

Catalytic activity of GRK2/3 is essential for the recruitment of β-arrestin2 by CB1R

Phosphorylation of GPCRs results in β-arrestin recruitment. In cells expressing β-arrestin2-Rluc with CB1R-YFP **(Suppl. Fig. 1C)**, a BRET signal increase was evident upon CB1R activation by WIN. This increase was obliterated upon the pretreatment of the cells with cmpd101 (mBRET values ± SEM in 10 minutes: CB1R = 29.72 ± 3.57; CB1R + cmpd101 = 5.46 ± 2.08) **(Fig. 2C)**. We verified that cmpd101 did not affect the expression of CB1R-YFP **(Suppl. Fig. 3A)**. Thus, the recruitment of β-arrestin2 to agonist-stimulated CB1R is directly dependent on the catalytic activity of GRK2/3.

Formation of GRK3-Gβγ complexes is only partially influenced by CB1R phosphorylation state

In cells co-expressing GRK3-Rluc8 and $G\beta_2$-Flag, Gγ2-YFP **(Suppl. Fig. 1D)**, the application of 1 μM WIN caused a prompt increase of BRET signal **(Fig. 3A)**. Subsequently, we used the CB1R mutants to study whether GRK3 association with Gβγ subunits is affected by CB1R C-tail phosphorylation patterns. WIN stimulation of the CB1R_2A was followed by a rapid increase in BRET signal due to the formation of GRK3-Gβγ complexes (mBRET values ± SEM at 5 minute CB1R = 138.3 ± 1.93; CB1R_2A = 157.5 ± 7.42) **(Fig. 3B)**.

The stimulation of the CB1R_6A produced an increase in BRET efficiency, although to a lower extent of the WT CB1R activation-induced BRET response (mBRET values ± SEM at 5 minutes: CB1R = 138.3 ± 1.93; CB1R_6A = 91.77 ± 2.90) **(Fig. 3C)**. Interestingly, the same result was obtained with the CB1R_8A transfected cells (mBRET values ± SEM at 5 minutes: CB1R = 138.3 ± 1.93; CB1R_8A = 83.82 ± 10.57) **(Fig. 3D)** indicating that the two motifs play different roles in regulating the GRK3-Gβγ interaction.

These results suggest that GRK3-Gβγ interactions are only partially dependent on CB1R phosphorylation and that phosphorylation of the CB1R C-terminal motif is not required for GRK3-Gβγ interaction.

SGIP1 strengthens and prolongs GRK3-Gβγ association

We previously reported that SGIP1 increased interactions between CB1R and β arrestin2 (Hajkova *et al.* 2016). We now show that the CB1R-driven GRK3 interaction with Gβγ subunits is also increased and prolonged in the presence of SGIP1. Indeed, in cells co-expressing GRK3-Rluc8, Gγ-YFP, CB1R, WIN stimulation of CB1R was followed by a rapid increase in BRET signal due to the formation of GRK3-Gβγ complexes, that was significantly enhanced and prolonged in the presence of co-expressed SGIP1 (mBRET values ± SEM in 30 minutes: CB1R = 107.6 ± 9.73; CB1R + SGIP1 = 160.3 ± 13.91) **(Fig. 3A).**

We also tested whether different CB1R C-tail phosphorylation patterns affect the ability of SGIP1 to enhance GRK3-Gβγ association. Activation of CB1R_2A in the presence SGIP1 resulted in significantly prolonged BRET signal in comparison with BRET produced by cells without SGIP1 expression (mBRET values ± SEM in 60 minutes: CB1R_2A = 101.1 ± 5.92; CB1R_2A + SGIP1 = 185.3 ± 10.76) **(Fig. 3B).** Interestingly, the GRK3-Gβγ association was significantly augmented immediately

after stimulation of CB1R_6A when coexpressed with SGIP1 (mBRET values ± SEM in 5 minutes: CB1R_6A = 99.04 ± 12.50; CB1R_6A + SGIP1 = 162.6 ± 10.40) **(Fig. 3C).** In cells expressing CB1R_8A, the dynamics of the association between GRK3-Gβγ after WIN stimulation was reminiscent of that without SGIP1 coexpression **(Fig. 3D).** The expression of Gγ-YFP or GRK3-Rluc8 was not modified when coexpressed with SGIP1-mCherry **(Suppl. Fig. 4G-I).**

SGIP1 therefore enhances the interaction between GRK3 and Gβγ that occurs during CB1R desensitization.

The two C-terminal motifs differentially control GRK3-CB1R interaction

We next studied the relationship between the phosphorylation pattern of CB1R and the recruitment of GRK3 **(Suppl. Fig. 1A)**. In cells co-expressing GRK3-Rluc8 and CB1R-YFP, the application of 1 µM WIN resulted in a rapid increase of BRET signal **(Fig. 4A)**.

We observed that preventing phosphorylation of the short motif ^{456}SMGDS^{429} increased and prolonged the interaction with GRK3 as the agonist stimulation of CB1R_2A-YFP resulted in a greater BRET signal between the receptor and GRK3-Rluc8 compared to the CB1R1-YFP/GRK3-Rluc8 pair (mBRET values ± SEM in 5 minutes: CB1R = 35.54 ± 2.26; CB1R_2A = 48.62 ± 4.82) **(Fig. 4B)**. The recruitment kinetic profile by activated CB1R_2D-YFP was similar to that obtained with the CB1R-YFP (CB1R = 35.54 ± 2.26; CB1R_2D = 31.69 ± 3.75) **(Supp. Fig. 5B).** This suggests that phosphorylation of the short motif may cause GRK3 dissociation from CB1R.

Interestingly, a much lower BRET signal was observed in cells expressing CB1R_6A-YFP (mutation of the serine/threonine residues of the motif ^{460}TMSVSTDTS^{468}) (mBRET values ± SEM in 5 minutes: CB1R = 35.54 ± 2.261; CB1R_6A = 12.36 ± 2.26) **(Fig. 4C)**. The response was abolished in presence of CB1R-8A **(Fig. 4D)**. This means that the phosphorylation of the long motif of ^{460}TMSVSTDTS^{468} is required for GRK3-CB1R interaction. This was confirmed by the fact that replacing the same residues by aspartate lead to BRET responses similar to that obtained with the WT CB1R. (mBRET values ± SEM in 5 minutes: CB1R = 35.54 ± 2.26; CB1R_6D = 27.50 ± 2.68; CB1R_8D = 18.62 ± 2.16) **(Supp. Fig. 5B).**

Expression of the mutated receptors was similar to that of wildtype CB1R and the expression of GRK3-Rluc8 was not modified by coexpression with any of the mutated receptors **(Suppl. Fig. 3B & C).**

SGIP1 enhances CB1R-GRK3 association

Interestingly, SGIP1, known to increase increased CB1R-β-arrestin2 interaction (Hajkova *et al.* 2016), also favored CB1R-GRK3 interaction. In HEK293 cells coexpressing CB1R-YFP variants, GRK3-Rluc8 and either SGIP1-mCherry or an empty vector pRK6, activation of CB1R in the presence of SGIP1 resulted in a significantly stronger and prolonged GRK3 recruitment (mBRET values ± SEM in 5 minutes: CB1R = 23.62 ± 3.54; CB1R + SGIP1 = 40.16 ± 2.01) **(Fig. 4A)**. SGIP1 further increases interaction of CB1R_2A with GRK3-RLuc8 (mBRET values ± SEM in 10 minutes: CB1R_2A = 63.56 ± 6.28; CB1R_2A + SGIP1 = 87.26 ± 3.92) **(Fig. 4B)**, but could not rescue the interaction between either CB1R_6A or CB1R_8A and GRK3 **(Fig. 4C & D).** The expression of the receptor mutants or GRK3-Rluc8 was not affected when coexpressed with SGIP1-mCherry **(Suppl. Fig. 4A-C)**.

These results suggest that SGIP1 strengthens and prolongs GRK3 recruitment to CB1R.

Phosphorylation of the CB1R C-tail regulates β-arrestin2 interaction

As expected, when the second motif cannot be phosphorylated, not only is GRK3 recruitment to CB1R lost, but the recruitment of β-arrestin2 is also prevented. Indeed, upon WIN stimulation, both CB1R_2A-YFP and CB1R_2D-YFP mutants were able to recruit β-arrestin2-Rluc, however to a significantly decreased extent in comparison to wildtype CB1R (mBRET values ± SEM in 5 minutes: CB1R = 29.33 ± 1.93; CB1R_2A = 15.53 ± 3.28; CB1R_2D = 18.48 ± 2.96) **(Fig. 5B and Suppl. Fig. 5C)**.

On the other hand, activation of CB1R_6A and CB1R_8A mutants resulted in severely impaired β-arrestin2 recruitment (mBRET values ± SEM in 5 minutes: CB1R = 29.33 ± 1.93; CB1R_6A = 3.49 ± 2.77; CB1R_8A = 4.28 ± 2.24) **(Fig. 5C & D)**. The expression of β-arrestin2-Rluc was not modified by the coexpression of the mutated receptors **(Suppl. Fig. 4D & E)**.

These results show that serine residues of the ^{456}SMGDS^{429} motif alone are not sufficient to mediate the optimal association of the CB1R with β-arrestin2, while the serine residues within ^{460}TMSVSTDTS^{468} region are required for β-arrestin2 recruitment.

SGIP1 strengthens the formation of CB1R-β-arrestin2 complexes in β-arrestin2-interacting receptors

As observed for GRK3-CB1R interaction, SGIP1 could increase the interaction between β-arrestin2 and CB1R (mBRET values ± SEM in 10 minutes: CB1R = 26.59 ± 7.08; CB1R + SGIP1 = 60.39 ± 3.53) **(Fig. 5A)** even if the short ^{456}SMGDS^{429} motif serine/threonine residues are mutated (mBRET values ± SEM in 10 minutes: CB1R_2A = 12.6 ± 3.60; CB1R_2A + SGIP1 = 30.30 ± 1.651) **(Fig. 5B**). In contrast, SGIP1 did not recover β-arrestin2 recruitment to CB1R_6A and CB1R_8A that contains the non-phosphorylatable long motif, ^{460}TMSVSTDTS^{468} **(Fig. 5C & D).** As a control to the above experiments, we verified the equivalent expression levels of receptors, β-arrestin2-Rluc and SGIP1-mCherry **(Suppl. Fig. 4D-F).**

These results suggest that SGIP1 strengthens and prolongs β-arrestin2 recruitment to the mutated receptors if recruitment occurs, but SGIP1 alone is insufficient for this interaction.

GRK3 and β-arrestin2 interaction with CB1R is regulated by different phosphorylation patterns of its C-tail

We created additional CB1R-YFP mutants within both the short and the long motifs in order to more precisely identify the residues involved for GRK3 and arrestin recruitment to CB1R **(Fig. 6A)**. The mutant CB1R_^{456}SMGDS^{429}_^{460}AMSVSADAS^{468} (with all threonines mutated into alanine residues) interacted with GRK3 with a similar profile as the wildtype receptor up to the peak at 5 min, but at later time points the BRET signal for this mutant was prolonged compared to wildtype CB1R **(Fig. 6B)**. Thus, CB1R_^{456}SMGDS^{429}_^{460}AMSVSADAS^{468} produced longer, or a spatially different association with GRK3 than wildtype CB1R (mBRET values ± SEM in 30 minutes: CB1R = 8.82 ± 4.03; CB1R_^{456}SMGDS^{429}_^{460}AMSVSADAS^{468} = 27.11 ± 3.71). This effect was further increased by mutation of the serines of the short motif (as observed above) **(Fig. 6B).**

In the next set of experiments, we used CB1R with mutated serine residues within the ^{456}SMGDS^{429} and at the same time, all the threonine residues in the distal C-terminus were mutated into alanine

residues, yielding CB1R_^{456}AMGDA^{429}_^{460}AMSVSADAS^{468}. This mutant receptor has an even more robust and profoundly extended association with GRK3 compared to wildtype receptor (mBRET values ± SEM in 30 minutes: CB1R = 8.82 ± 4.03; CB1R_^{456}AMGDA^{429}_^{460}AMSVSADAS^{468} = 48.58 ± 2.34) **(Fig. 6B)**. This further confirms that serine residues phosphorylation within the ^{456}SMGDS^{429} is important for the dissociation of GRK3 from CB1R likely in addition to the role of the threonine residues in the long motif.

In contrast, as expected according to the loss of GRK recruitment by CB1R-6A or 8A, the CB1R_^{456}SMGDS^{429}_^{460}TMAVATDTA^{468} mutant had a reduced ability to recruit GRK3 compared to CB1R (mBRET values ± SEM in 5 minutes: CB1R = 51.69 ± 2.04; CB1R_^{456}SMGDS^{429}_^{460}TMAVATDTA^{468} = 28.95 ± 2.18). Interestingly, parallel mutations of the serine residues in the case of CB1R_^{456}AMGDA^{429}_^{460}TMAVATDT^{A468} mutant further reduced GRK3 association (mBRET values ± SEM in 5 minutes: CB1R = 51.69 ± 2.04; CB1R_^{456}AMGDA^{429}_^{460}TMAVATDTA^{468} = 13.81 ± 2.03) **(Fig. 6B)**. The expression of the mutant receptors was similar to that of the CB1R **(Suppl. Fig. 3F)**. This confirms that the serine residues of ^{460}TMSVSTDTS^{468} motif are crucial for GRK3 recruitment or for its strong interaction with CB1R.

We detected only a marginal interaction of these four CB1R mutants with β-arrestin2 **(Fig. 6C).** Therefore, precise and extensive phosphorylation of both motifs is required for optimal interaction of CB1R with β-arrestin2. Phosphorylation of most residues within the second motif is required, as their mutation suppressed completely the receptor-β-arrestin2 interaction.

Discussion

This study describes previously unknown molecular mechanisms and interactions of molecules following the activation of the CB1R as in undergoes desensitization. The kinase activity of GRK2/3 orchestrates GRK3's interaction with G protein Gβγ subunits as well as with the receptor, leading to the phosphorylation of several residues within CB1R C-terminal tail. We aimed at dissecting the specificity of the phosphorylation patterns to drive selected interactions within the signalosome that results in desensitization of CB1R. We also show that SGIP1, a recently detected CB1R interacting partner, has profound effects on the extent and kinetics of the signalosome.

GRK2/3 activation is a key step in CB1R desensitization

GRK2/3s execute a significant step in the desensitization of numerous GPCRs (Luo *et al.* 2017; Dautzenberg *et al.* 2002; Dautzenberg & Hauger 2001; Bawa *et al.* 2003; Appleyard *et al.* 1999; Ishii *et al.* 1994; Celver *et al.* 2001). Activation of G proteins recruits GRK2/3 via an interaction with G protein Gβγ dimer and fosters association between GRK2/3 and the receptor, which is consequently phosphorylated within its intracellular C terminus by the kinase (Homan & Tesmer 2015; Nogues *et al.* 2017). Desensitization of CB1R expressed in Xenopus oocytes was shown to be dependent on the presence of both GRK3 and β-arrestin2 (Daigle *et al.* 2008a; Daigle *et al.* 2008b; Gyombolai *et al.* 2013). Our data are in accord with these findings: the kinase activity of GRK2/3 is essential for efficient β-arrestin2 recruitment to CB1R.

GRK3-Gβγ interaction

Cmpd101 interacts with GRK2 and GRK3 in their noncatalytic form and blocks their activation by binding to the active site (Ikeda S 2007; Thal *et al.* 2011). Following receptor activation, GRK2/3 interacts with the membrane-associated Gβγ dimers (Touhara *et al.* 1994; Daaka *et al.* 1997; Boughton *et al.* 2011). In our experiments, cmpd101 inhibited the interaction of GRK3 with G protein βγ dimer, albeit not completely **(Fig. 2A).** Thus, GRK3 also has to be in the active state in order to fully interact with the Gβγ dimer. Partial interaction between GRK3-Gβγ, even upon the presence of the GRK3 inhibitor following CB1R activation can be either result of incomplete inhibition of the GRK3 by cmpd101, or residual affinity between pleckstrin homology domain of inactive GRK3 and the released Gβγ (Lodowski *et al.* 2003). Interestingly, to a large extent, GRK3 was able to form complexes with Gβγ independently of CB1R C-tail phosphorylation patterns. Furthermore, GRK3-Gβγ association is enhanced by SGIP1. Thus, despite the release of Gβγ protein from the trimeric G protein, following its activation, these molecules participate in the CB1R interactome.

GRK3-CB1R association

In the presence of cmpd101, recruitment of GRK3 to CB1R is blocked **(Fig. 2B)**, demonstrating that GRK3 has to be in an active conformation to interact with the activated CB1R. The residues on the CB1R C-tail that undergo GRK2/3 driven phosphorylation are distributed in two clusters, ^{456}SMGDS^{429} and ^{460}TMSVSTDTS^{468}. GRK3/CB1R recruitment assays with serine/threonine residues mutated within these regions to alanine residues identified two major findings. Firstly, stimulation of CB1R_2A (S456A, S429A mutations) resulted in significantly enhanced and prolonged GRK3

association, compared to the wild type CB1R. Mutagenesis within the ^{460}TMSVSTDTS^{468} motif in CB1R_6A resulted only in partial attenuation of GRK3 recruitment to the receptor. Mutation of all serine/threonine residues to alanine within both, ^{456}SMGDS^{429} and ^{460}TMSVSTDTS^{468} regions (CB1R_8A) abrogated GRK3 recruitment to the activated receptor **(Fig. 4D).** The GRK3 recruitment profile of the CB1R_2D mutant, in which Aspartate residues mimic the phosphorylated state (S423D, S429D), resembled that of CB1R WT **(Suppl. Fig. 5B).** Replacement of serine/threonine residues within the ^{460}TMSVSTDTS^{468} region to aspartates only partially rescued the WT CB1R-GRK3 dynamics **(Suppl. Fig. 5B)**. This might be due to the fact that phosphoserine modification contains double negative charges, while aspartic acid has only a single charge, and perhaps this is insufficient for proper GRK3 binding. Also, phosphorylation of the residues is a dynamic process, and this is not reflected by the use of the constitutively charged aspartic acid in the corresponding CB1R mutants.

Based on these observations we propose a hypothesis that phosphorylation of residues within the ^{456}SMGDS^{429} region by GRK3 regulates the dynamics of GRK3-CB1R association. Following their interaction, phosphorylation of residues within ^{460}TMSVSTDTS^{468} region favors the association, but subsequent phosphorylation of residues from ^{456}SMGDS^{429} in turn expedites the dissociation of GRK3. This averts spatial hindrance and allows β-arrestin2 association with the receptor. SGIP1 also modifies CB1R association with GRK3, with enhanced impact on their transient interaction in later phases of the desensitization **(Fig. 4A)**. This finding further underlines the role of the CB1R-SGIP1 association on the dynamics of the interactions within the signalosome during CB1R desensitization.

CB1R-β-arrestin2 interaction

Upon treatment with cmpd101, recruitment of β-arrestin2 to the activated CB1R was significantly constrained **(Fig. 2C).** We attribute this inhibition of β-arrestin2 recruitment to the inhibition of GRK2/3 activation impairing CB1R phosphorylation. Previously, using quantitative analysis of fluorescent confocal images, mutant CB1R_2A (mutations of serine residues within the ^{456}SMGDS^{429} motif named CB1R S456A/S429A in the preceding study) recruited β-arrestin-2 to the plasma membrane (Daigle *et al.* 2008a). We revealed an impaired association of β-arrestin-2 with this mutant **(Fig. 5A).** Therefore, both CB1R, and the mutated CB1R_2A mobilize β-arrestin2 from the cytoplasm to the plasmalemma, however, our data show that levels of protein-protein association of β-arrestin2 are decreased in the case of CB1R_2A. The aforementioned study used quantitative analysis of fluorescent confocal images that reveal recruitment from the cytoplasm towards the membrane, while BRET technology allows more specific depiction of protein-protein interactions. A possibility exists that CB1R_2A-β-arrestin2 complex acquires a different conformational state than with the wildtype receptor, decreasing BRET signal efficiency (Cahill *et al.* 2017; Nuber *et al.* 2016). Phosphorylation of residues within the ^{456}SMGDS^{429} and ^{460}TMSVSTDTS^{468} region in CB1R_8A impaired CB1R mediated translocation of β-arrestin2 to the membrane, and their mutation to alanine residues prevented internalization (Daigle *et al.* 2008b; Jin *et al.* 1999) **(Fig. 5D).** Here, our data are in agreement with the previous report, in which mutation of all eight phosphorylation sites results in loss of the ability to recruit β-arrestin2 from the cytoplasm.

Our observations support the hypothesis that the ^{460}TMSVSTDTS^{468} motif serves as an initiation docking site for β-arrestin2 (Blume *et al.* 2017; Jin *et al.* 1999; Morgan *et al.* 2014). We hypothesize that the decreased β-arrestin2 interaction with CB1R_2A is a consequence of protracted GRK3-CB1R_2A interaction. Due to higher affinity between GRK3 and CB1R_2A and GRK3, this kinase sterically hinders β-arrestin2 interaction with the CB1R_2A.

Previously, we described the impact of SGIP1 on the CB1R- β-arrestin-2 association. Here we detected that SGIP1 restored β-arrestin2 interaction with CB1R_2A **(Fig. 5 B)**. This further points to the specificity of functional consequences of SGIP1-CB1R interaction.

GRK3 and β-arrestin2 interactions with CB1R depend on unique phosphorylation patterns

To further explore the phosphorylation patterns needed for the interaction between CB1R and GRK3, or β-arrestin2, we constructed additional CB1R mutants with several combinations of alanine replacements within ^{460}TMSVSTDTS^{468} region. The substitution of only serine residues with alanine residues decreased the receptor's ability to recruit GRK3. In contrast, mutation of all threonine into alanine residues within the same region resulted in a mutant with extended CB1R-GRK3 association. This was even more significant if S456A and S429A mutations were also included **(Fig. 6B)**. These results further illustrate that phosphorylation of ^{456}SMGDS^{429} drives dissociation of GRK3 from the receptor. In contrast, phosphorylation of serine residues within the ^{460}TMSVSTDTS^{468} region is crucial for the formation of CB1R-GRK3 complexes. Conversely, the substitution of the threonine by alanine residues within this region did not prevent the CB1R-GRK3 association, suggesting that phosphorylation of threonine residues are not indispensable for the GRK3 association.

All the CB1R variants with different triple alanine mutations in the extreme C-tail exhibited similarly decreased, but not completely diminished, recruitment of β-arrestin2 **(Fig. 5C).** Hence, serine and threonine residues within ^{460}TMSVSTDTS^{468} motif, all contribute to β-arrestin2 recruitment. This contrasts with the phosphorylation pattern needed for the GRK3-CB1R interaction. Of importance, depending on certain phosphorylation patterns, β-arrestins can acquire a wide range of conformation states. These different conformations, imposed by distinct phosphorylation patterns of the C termini, may also lead to differential BRET efficiencies (Latorraca *et al.* 2020; Nuber *et al.* 2016; Lee *et al.* 2016; Nobles *et al.* 2011). Our results may also point to sequential and/or cumulative phosphorylation of serine/threonine residues in ^{460}TMSVSTDTS^{468} of CB1R, as those dynamics may orchestrate β-arrestin2 recruitment.

The μ-opioid receptor also has a clustering of serine/threonine residues within two regions. Meiss and colleagues described that phosphorylation of two serine/threonine clusters within the C-terminal region of the μ-opioid receptor controls the dynamics of GRK2 and β-arrestin2 recruitment (Miess *et al.* 2018). The extreme C-tail serine/threonine cluster was involved in GRK2 and β-arrestin2 recruitment, while the proximal serine/threonine region was involved in the stability of these interactions. Our data harmonize with those findings. GRK3 and β-arrestin2 interactions with CB1R are regulated by different phosphorylation patterns of the receptor C-tail. A recent study performed by Møller and colleagues disclosed that in the case of the μ-opioid receptor, GRK2 and GRK3 have distinct impacts on β-arrestin2 association (Moller *et al.* 2020), pointing to the complexity of the process, and likely to unique particulars of the desensitization process of different receptors.

SGIP1 augments GRK3-Gβγ, GRK3-CB1R, and β-arrestin2-CB1R interactions

Previously, we described that G protein activation by CB1R is not affected by SGIP1. Subsequent events dependent on CB1R C-tail phosphorylation that would result in clathrin-mediated endocytosis (CME) are profoundly impeded by SGIP1. SGIP1 stalls CME, and the phosphorylated receptor remains on the cell surface. We proposed a hypothesis that aims at depicting how the relationship between SGIP1 and CB1R affects events that follow CB1R desensitization; During CB1R

desensitization, β-arrestins interact with the phosphorylated CB1R. The temporary association between phosphorylated CB1R and β-arrestin terminates as the receptor is internalized. SGIP1 stalls CB1R internalization. Therefore, the β-arrestin interaction with desensitized CB1R persists longer in the presence of SGIP1. The consequence of stabilizing CB1R at the cell surface by SGIP1 is that dissociation of β-arrestin2 from CB1R that follows internalization occurs more slowly, as depicted in our earlier study (Hajkova *et al.* 2016).

The interaction of GRK3 with Gβγ subunits following activation of the CB1R was also modified by SGIP1 in this study **(Fig. 3, Fig. 7)**. Interestingly, the most evident effect of SGIP1 on the dynamics of this protein-protein association is at the early phase, and persist through the observed period. Also, we show that the presence of SGIP1 results in enhancement of GRK3 association with both CB1R and CB1R_2A, but not with CB1R_6A, and CB1R_8A mutants that lose the ability to associate with GRK3 and β-arrestin2 **(Fig. 4 C-D, Fig. 5 C-D)**.

SGIP1 modifies most of the interactions within the CB1R desensitization interactome **(Fig. 7 C)**. This indicates that the C-tail phosphorylation patterns of CB1R does not affect SGIP1 association with CB1R. This is in agreement with our previous observations using yeast two hybrid screen with mutated C terminus of CB1R mimicking phosphorylated state of the residues. Using such mutants did not have any effect on the association between CB1R and SGIP1 (Fig. 1 A in (Hajkova *et al.* 2016)). Therefore, CB1R association with SGIP1 is independent of the modification, but perhaps, SGIP1 influences the phosphorylation patterns of CB1R during desensitization.

Conclusion

GRK3 has to reach an active conformation in order to fully interact with Gβγ dimer and CB1R to phosphorylate the CB1R C-tail. . The interaction of GRK3 and Gβγ is allosterically modulated by the CB1R-GRK3 complex and by SGIP1. Phosphorylation of Serine residues within the ^{456}SMGDS^{429} region by GRK3 causes relaxation of the GRK3-CB1R association. The phosphorylation arrangement, called a “bar code” of serine/threonine residues within ^{460}TMSVSTDTS^{468} region, required for the receptor to interact with GRK3 and β-arrestin2, has distinct implications. Alike in case of CB1R interaction with β-arrestin, SGIP1 enhances the association of GRK3 with both, Gβγ subunits of G proteins and CB1R. Therefore, SGIP1 regulates levels of interactions between molecules that are part of the temporal CB1R signalosome that organizes during its desensitization.

Conflicts of interest

All authors report no biomedical financial interests or potential conflicts of interest.

Acknowledgments

This project was supported by Grant Agency of Czech Republic (19-24172S), LM2015040 (Czech Centre for Phenogenomics) and by RVO: 68378050-KAV-NPUI by the Czech Academy of Sciences. Some pharmacology and BRET experiments were performed using the ARPEGE Pharmacology-Screening-Interactome platform facility (UMS Biocampus), Montpelier, France. For help with editing the text, we are thankful to Anna Karimova.

Author’s Contributions

Matej Gazdarica, Laurent Prezeau, Jaroslav Blahos designed research; Matej Gazdarica, Judith Noda performed research; Ken Mackie contributed new reagents or analytic tools; Matej Gazdarica, Oleh Duridyvka, Vendula Novosadova, Jean-Philippe Pin, Laurent Prezeau, Jaroslav Blahos analysed data; and Matej Gazdarica, Ken Mackie, Laurent Prezeau, Jaroslav Blahos wrote the paper.

References

Al-Zoubi, R., Morales, P. and Reggio, P. H. (2019) Structural Insights into CB1 Receptor Biased Signaling. *International Journal of Molecular Sciences* **20**.

Appleyard, S. M., Celver, J., Pineda, V., Kovoor, A., Wayman, G. A. and Chavkin, C. (1999) Agonist-dependent desensitization of the kappa opioid receptor by G protein receptor kinase and beta-arrestin. *J Biol Chem* **274,** 23802-23807.

Araque, A., Castillo, P. E., Manzoni, O. J. and Tonini, R. (2017) Synaptic functions of endocannabinoid signaling in health and disease. *Neuropharmacology* **124,** 13-24.

Bakshi, K., Mercier, R. W. and Pavlopoulos, S. (2007) Interaction of a fragment of the cannabinoid CB1 receptor C-terminus with arrestin-2. *FEBS Lett* **581,** 5009-5016.

Bawa, T., Altememi, G. F., Eikenburg, D. C. and Standifer, K. M. (2003) Desensitization of alpha 2A-adrenoceptor signalling by modest levels of adrenaline is facilitated by beta 2-adrenoceptor-dependent GRK3 up-regulation. *Br J Pharmacol* **138,** 921-931.

Blume, L. C., Patten, T., Eldeeb, K. et al. (2017) Cannabinoid Receptor Interacting Protein 1a Competition with beta-Arrestin for CB1 Receptor Binding Sites. *Mol Pharmacol* **91,** 75-86.

Boughton, A. P., Yang, P., Tesmer, V. M., Ding, B., Tesmer, J. J. and Chen, Z. (2011) Heterotrimeric G protein beta1gamma2 subunits change orientation upon complex formation with G protein-coupled receptor kinase 2 (GRK2) on a model membrane. *Proc Natl Acad Sci U S A* **108,** E667-673.

Brule, C., Perzo, N., Joubert, J. E., Sainsily, X., Leduc, R., Castel, H. and Prezeau, L. (2014) Biased signaling regulates the pleiotropic effects of the urotensin II receptor to modulate its cellular behaviors. *FASEB J* **28,** 5148-5162.

Cahill, T. J., 3rd, Thomsen, A. R., Tarrasch, J. T. et al. (2017) Distinct conformations of GPCR-beta-arrestin complexes mediate desensitization, signaling, and endocytosis. *Proc Natl Acad Sci U S A* **114,** 2562-2567.

Carman, C. V., Barak, L. S., Chen, C., Liu-Chen, L. Y., Onorato, J. J., Kennedy, S. P., Caron, M. G. and Benovic, J. L. (2000) Mutational analysis of Gbetagamma and phospholipid interaction with G protein-coupled receptor kinase 2. *J Biol Chem* **275,** 10443-10452.

Celver, J. P., Lowe, J., Kovoor, A., Gurevich, V. V. and Chavkin, C. (2001) Threonine 180 is required for G-protein-coupled receptor kinase 3- and beta-arrestin 2-mediated desensitization of the mu-opioid receptor in Xenopus oocytes. *J Biol Chem* **276,** 4894-4900.

Charest, P. G. and Bouvier, M. (2003) Palmitoylation of the V2 vasopressin receptor carboxyl tail enhances beta-arrestin recruitment leading to efficient receptor endocytosis and ERK1/2 activation. *J Biol Chem* **278,** 41541-41551.

Daaka, Y., Pitcher, J. A., Richardson, M., Stoffel, R. H., Robishaw, J. D. and Lefkowitz, R. J. (1997) Receptor and G betagamma isoform-specific interactions with G protein-coupled receptor kinases. *Proc Natl Acad Sci U S A* **94,** 2180-2185.

Daigle, T. L., Kearn, C. S. and Mackie, K. (2008a) Rapid CB1 cannabinoid receptor desensitization defines the time course of ERK1/2 MAP kinase signaling. *Neuropharmacology* **54,** 36-44.

Daigle, T. L., Kwok, M. L. and Mackie, K. (2008b) Regulation of CB1 cannabinoid receptor internalization by a promiscuous phosphorylation-dependent mechanism. *J Neurochem* **106,** 70-82.

Dautzenberg, F. M. and Hauger, R. L. (2001) G-protein-coupled receptor kinase 3- and protein kinase C-mediated desensitization of the PACAP receptor type 1 in human Y-79 retinoblastoma cells. *Neuropharmacology* **40,** 394-407.

Dautzenberg, F. M., Wille, S., Braun, S. and Hauger, R. L. (2002) GRK3 regulation during CRF- and urocortin-induced CRF1 receptor desensitization. *Biochem Biophys Res Commun* **298,** 303-308.

de Jesus, M. L., Salles, J., Meana, J. J. and Callado, L. F. (2006) Characterization of CB1 cannabinoid receptor immunoreactivity in postmortem human brain homogenates. *Neuroscience* **140,** 635-643.

Dvorakova, M., Kubik-Zahorodna, A., Straiker, A., Sedlacek, R., Hajkova, A., Mackie, K. and Blahos, J. (2021) SGIP1 is involved in regulation of emotionality, mood, and nociception and tunes in vivo signaling of Cannabinoid Receptor 1. *Br J Pharmacol*.

Fletcher-Jones, A., Hildick, K. L., Evans, A. J., Nakamura, Y., Henley, J. M. and Wilkinson, K. A. (2020) Protein Interactors and Trafficking Pathways That Regulate the Cannabinoid Type 1 Receptor (CB1R). *Front Mol Neurosci* **13,** 108.

Garcia, D. E., Brown, S., Hille, B. and Mackie, K. (1998) Protein kinase C disrupts cannabinoid actions by phosphorylation of the CB1 cannabinoid receptor. *J Neurosci* **18,** 2834-2841.

Gurevich, E. V., Tesmer, J. J., Mushegian, A. and Gurevich, V. V. (2012) G protein-coupled receptor kinases: more than just kinases and not only for GPCRs. *Pharmacol Ther* **133,** 40-69.

Gyombolai, P., Boros, E., Hunyady, L. and Turu, G. (2013) Differential beta-arrestin2 requirements for constitutive and agonist-induced internalization of the CB1 cannabinoid receptor. *Mol Cell Endocrinol* **372,** 116-127.

Hajkova, A., Techlovska, S., Dvorakova, M., Chambers, J. N., Kumpost, J., Hubalkova, P., Prezeau, L. and Blahos, J. (2016) SGIP1 alters internalization and modulates signaling of activated cannabinoid receptor 1 in a biased manner. *Neuropharmacology* **107,** 201-214.

Haring, M., Marsicano, G., Lutz, B. and Monory, K. (2007) Identification of the cannabinoid receptor type 1 in serotonergic cells of raphe nuclei in mice. *Neuroscience* **146,** 1212-1219.

Herkenham, M., Lynn, A. B., Little, M. D., Johnson, M. R., Melvin, L. S., de Costa, B. R. and Rice, K. C. (1990) Cannabinoid receptor localization in brain. *Proc Natl Acad Sci U S A* **87,** 1932-1936.

Homan, K. T. and Tesmer, J. J. (2015) Molecular basis for small molecule inhibition of G protein-coupled receptor kinases. *ACS Chem Biol* **10,** 246-256.

Hsieh, C., Brown, S., Derleth, C. and Mackie, K. (1999) Internalization and recycling of the CB1 cannabinoid receptor. *J Neurochem* **73,** 493-501.

Ikeda S, K. M., Fujiwara S (2007) Cardiotonic agent comprising GRK inhibitor. (T. P. C. Ltd ed.). Ikeda S, Keneko M, and Fujiwara S, Japan.

Ishii, K., Chen, J., Ishii, M., Koch, W. J., Freedman, N. J., Lefkowitz, R. J. and Coughlin, S. R. (1994) Inhibition of thrombin receptor signaling by a G-protein coupled receptor kinase. Functional specificity among G-protein coupled receptor kinases. *J Biol Chem* **269,** 1125-1130.

Jin, W., Brown, S., Roche, J. P., Hsieh, C., Celver, J. P., Kovoor, A., Chavkin, C. and Mackie, K. (1999) Distinct domains of the CB1 cannabinoid receptor mediate desensitization and internalization. *J Neurosci* **19,** 3773-3780.

Katona, I. and Freund, T. F. (2012) Multiple functions of endocannabinoid signaling in the brain. *Annu Rev Neurosci* **35,** 529-558.

Kirilly, E., Hunyady, L. and Bagdy, G. (2013) Opposing local effects of endocannabinoids on the activity of noradrenergic neurons and release of noradrenaline: relevance for their role in depression and in the actions of CB1 receptor antagonists. *J Neural Transm* **120,** 177-186.

Koch, W. J., Inglese, J., Stone, W. C. and Lefkowitz, R. J. (1993) The binding site for the beta gamma subunits of heterotrimeric G proteins on the beta-adrenergic receptor kinase. *J Biol Chem* **268,** 8256-8260.

Latorraca, N. R., Masureel, M., Hollingsworth, S. A. et al. (2020) How GPCR Phosphorylation Patterns Orchestrate Arrestin-Mediated Signaling. *Cell* **183,** 1813-1825 e1818.

Lee, M. H., Appleton, K. M., Strungs, E. G., Kwon, J. Y., Morinelli, T. A., Peterson, Y. K., Laporte, S. A. and Luttrell, L. M. (2016) The conformational signature of beta-arrestin2 predicts its trafficking and signalling functions. *Nature* **531,** 665-668.

Leterrier, C., Bonnard, D., Carrel, D., Rossier, J. and Lenkei, Z. (2004) Constitutive endocytic cycle of the CB1 cannabinoid receptor. *Journal of Biological Chemistry* **279,** 36013-36021.

Liu, H. T. and Naismith, J. H. (2008) An efficient one-step site-directed deletion, insertion, single and multiple-site plasmid mutagenesis protocol. *Bmc Biotechnol* **8**.

Lodowski, D. T., Barnhill, J. F., Pyskadlo, R. M., Ghirlando, R., Sterne-Marr, R. and Tesmer, J. J. (2005) The role of G beta gamma and domain interfaces in the activation of G protein-coupled receptor kinase 2. *Biochemistry* **44,** 6958-6970.

Lodowski, D. T., Pitcher, J. A., Capel, W. D., Lefkowitz, R. J. and Tesmer, J. J. G. (2003) Keeping G proteins at bay: A complex between G protein-coupled receptor kinase 2 and G beta gamma. *Science* **300,** 1256-1262.

Luo, J., Busillo, J. M., Stumm, R. and Benovic, J. L. (2017) G Protein-Coupled Receptor Kinase 3 and Protein Kinase C Phosphorylate the Distal C-Terminal Tail of the Chemokine Receptor CXCR4 and Mediate Recruitment of beta-Arrestin. *Mol Pharmacol* **91,** 554-566.

Marsicano, G. and Lutz, B. (1999) Expression of the cannabinoid receptor CB1 in distinct neuronal subpopulations in the adult mouse forebrain. *Eur J Neurosci* **11,** 4213-4225.

Miess, E., Gondin, A. B., Yousuf, A. et al. (2018) Multisite phosphorylation is required for sustained interaction with GRKs and arrestins during rapid mu-opioid receptor desensitization. *Sci Signal* **11**.

Moller, T. C., Pedersen, M. F., van Senten, J. R., Seiersen, S. D., Mathiesen, J. M., Bouvier, M. and Brauner-Osborne, H. (2020) Dissecting the roles of GRK2 and GRK3 in mu-opioid receptor internalization and beta-arrestin2 recruitment using CRISPR/Cas9-edited HEK293 cells. *Sci Rep* **10,** 17395.

Moore, C. A. C., Milano, S. K. and Benovic, J. L. (2007) Regulation of receptor trafficking by GRKs and arrestins. *Annu Rev Physiol* **69,** 451-482.

Morgan, D. J., Davis, B. J., Kearn, C. S. et al. (2014) Mutation of putative GRK phosphorylation sites in the cannabinoid receptor 1 (CB1R) confers resistance to cannabinoid tolerance and hypersensitivity to cannabinoids in mice. *J Neurosci* **34,** 5152-5163.

Nobles, K. N., Xiao, K., Ahn, S. et al. (2011) Distinct phosphorylation sites on the beta(2)-adrenergic receptor establish a barcode that encodes differential functions of beta-arrestin. *Sci Signal* **4,** ra51.

Nogueras-Ortiz, C. and Yudowski, G. A. (2016) The Multiple Waves of Cannabinoid 1 Receptor Signaling. *Mol Pharmacol* **90,** 620-626.

Nogues, L., Reglero, C., Rivas, V., Neves, M., Penela, P. and Mayor, F., Jr. (2017) G-Protein-Coupled Receptor Kinase 2 as a Potential Modulator of the Hallmarks of Cancer. *Mol Pharmacol* **91,** 220-228.

Nuber, S., Zabel, U., Lorenz, K., Nuber, A., Milligan, G., Tobin, A. B., Lohse, M. J. and Hoffmann, C. (2016) beta-Arrestin biosensors reveal a rapid, receptor-dependent activation/deactivation cycle. *Nature* **531,** 661-664.

Pacher, P. and Kunos, G. (2013) Modulating the endocannabinoid system in human health and disease successes and failures. *Febs J* **280,** 1918-1943.

Pitcher, J. A., Inglese, J., Higgins, J. B. et al. (1992) Role of beta gamma subunits of G proteins in targeting the beta-adrenergic receptor kinase to membrane-bound receptors. *Science* **257,** 1264-1267.

Singh, S. N., Bakshi, K., Mercier, R. W., Makriyannis, A. and Pavlopoulos, S. (2011) Binding between a distal C-terminus fragment of cannabinoid receptor 1 and arrestin-2. *Biochemistry* **50,** 2223-2234.

Straiker, A., Wager-Miller, J. and Mackie, K. (2012) The CB1 cannabinoid receptor C-terminus regulates receptor desensitization in autaptic hippocampal neurones. *Br J Pharmacol* **165,** 2652-2659.

Thal, D. M., Yeow, R. Y., Schoenau, C., Huber, J. and Tesmer, J. J. (2011) Molecular mechanism of selectivity among G protein-coupled receptor kinase 2 inhibitors. *Mol Pharmacol* **80,** 294-303.

Touhara, K., Inglese, J., Pitcher, J. A., Shaw, G. and Lefkowitz, R. J. (1994) Binding of G-Protein Beta-Gamma-Subunits to Pleckstrin Homology Domains. *Journal of Biological Chemistry* **269,** 10217-10220.

Wager-Miller, J., Westenbroek, R. and Mackie, K. (2002) Dimerization of G protein-coupled receptors: CB1 cannabinoid receptors as an example. *Chem Phys Lipids* **121,** 83-89.

Xu, Y., Piston, D. W. and Johnson, C. H. (1999) A bioluminescence resonance energy transfer (BRET) system: application to interacting circadian clock proteins. *Proc Natl Acad Sci U S A* **96,** 151-156.

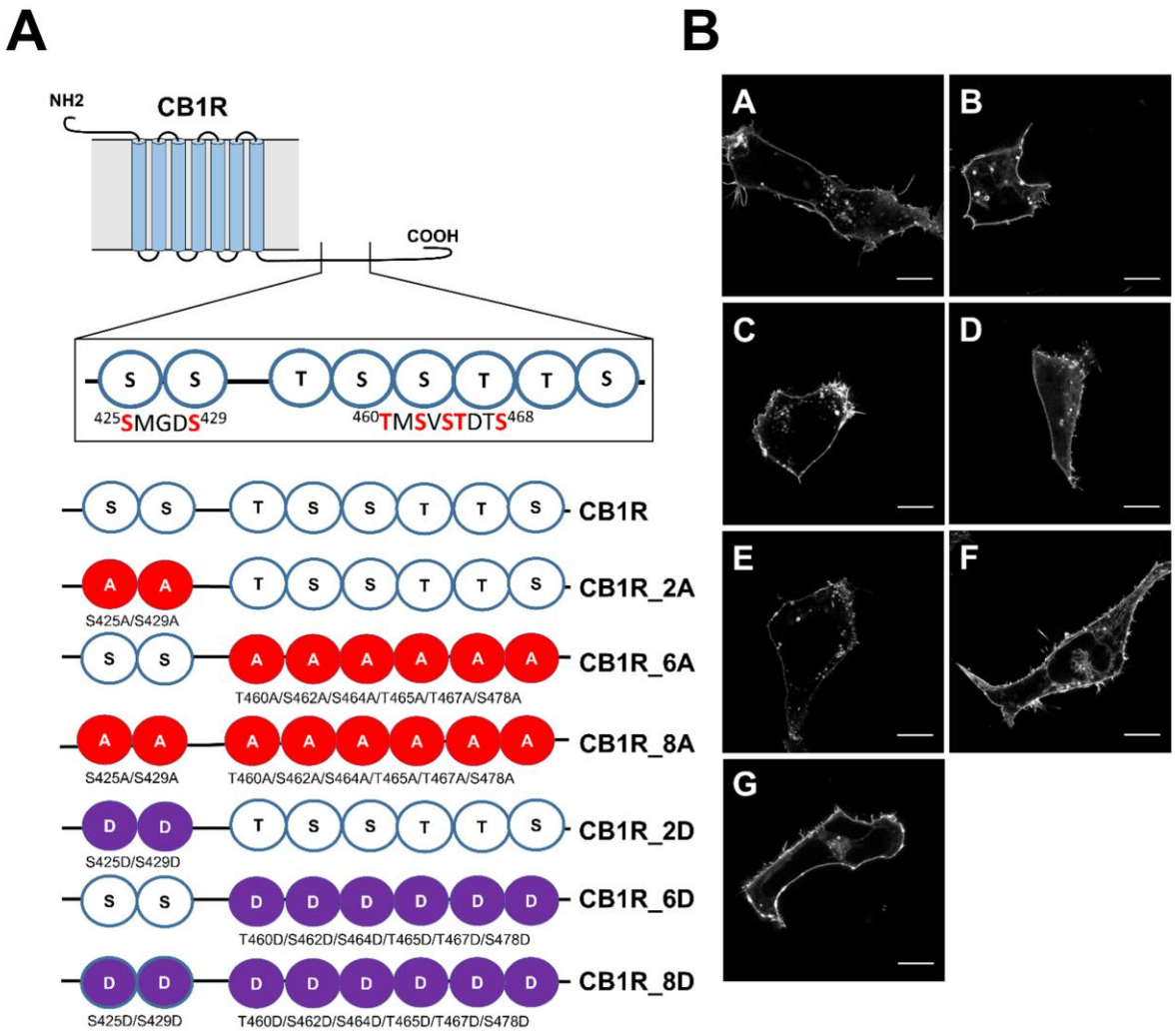

Fig. 1. Schematic depiction of CB1R mutants within the C-tail and characterization of their cellular distribution. ***A)*** *Two regions of CB1R:* ^{456}*SMGDS*^{429} *and* ^{460}*TMSVSTDTS*^{468} *contain serine/threonine residues that are likely to be involved in the desensitization and internalization of CB1R. CB1R C-tail phosphorylation mutants were created according to the scheme: A - mutation into alanine, D - mutation into aspartic acid.* ***B)*** *CB1R and mutant CB1Rs are predominantly localized on the cellular membrane. HEK293 cells were transiently transfected with CB1R-YFP variant. 24 hours after transfection, cells were visualized using fluorescent microscope. A single confocal section through the equatorial plane of the cells is shown. Legend: A) CB1R, B) CB1R_2A, C) CB1R_6A, D) CB1R_8A, E) CB1R_2D, F) CB1R_6D, G) CB1R_8D. Scale bar represents 10 µm.*

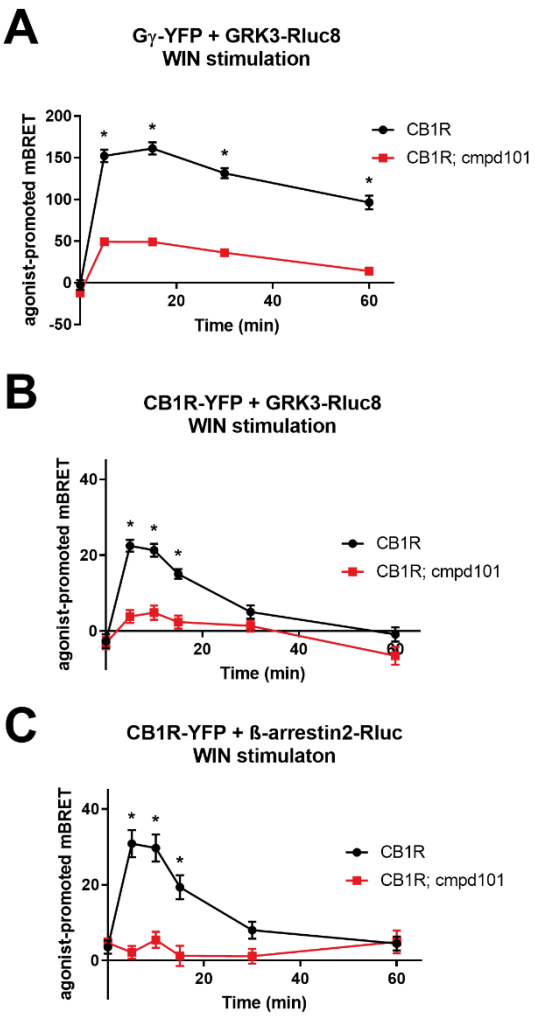

Fig. 2. Consequences of GRK3 inactivation on the protein-protein interactions. *HEK293 cells were transiently cotransfected with the following plasmid combinations: CB1R-YFP + GRK3-RLuc8 + empty plasmid pRK6 (2:1:2 ratio), CB1R-SNAP + GRK3-Rluc8 + Gβ-flag + Gγ-YFP (2:1:1:2 ratio) or CB1R-YFP + β-arrestin2-Rluc + empty plasmid pRK6 (2:1:2 ratio). After sixteen hours, cells were pretreated or not for 30 minutes with cmpd101 (30 µM) prior to stimulation with the CB1R agonist WIN55212-2 (WIN, 1 µM).* ***A)*** *Kinetic profiles of GRK3-RLuc8 and Gγ-YFP association dynamics in cmpd101 treated and non-treated cells.* ***B)*** *Kinetic profiles of GRK3-RLuc8 recruitment by WIN-activated CB1R-YFP in HEK293 cells pretreated or not with cmpd101.* ***C)*** *Kinetic profiles of β-arrestin2-Rluc recruitment by activated CB1R-YFP in cmpd101 pretreated and non-pretreated cells. Data represent the mean ± SEM of three expriments of independent cell preparations performed in 3 technical replicates and normalized against the maximal response of cmpd101 untreated cells. * represents p ≤ 0.05 (full statistical analysis is disclosed in Table 1).*

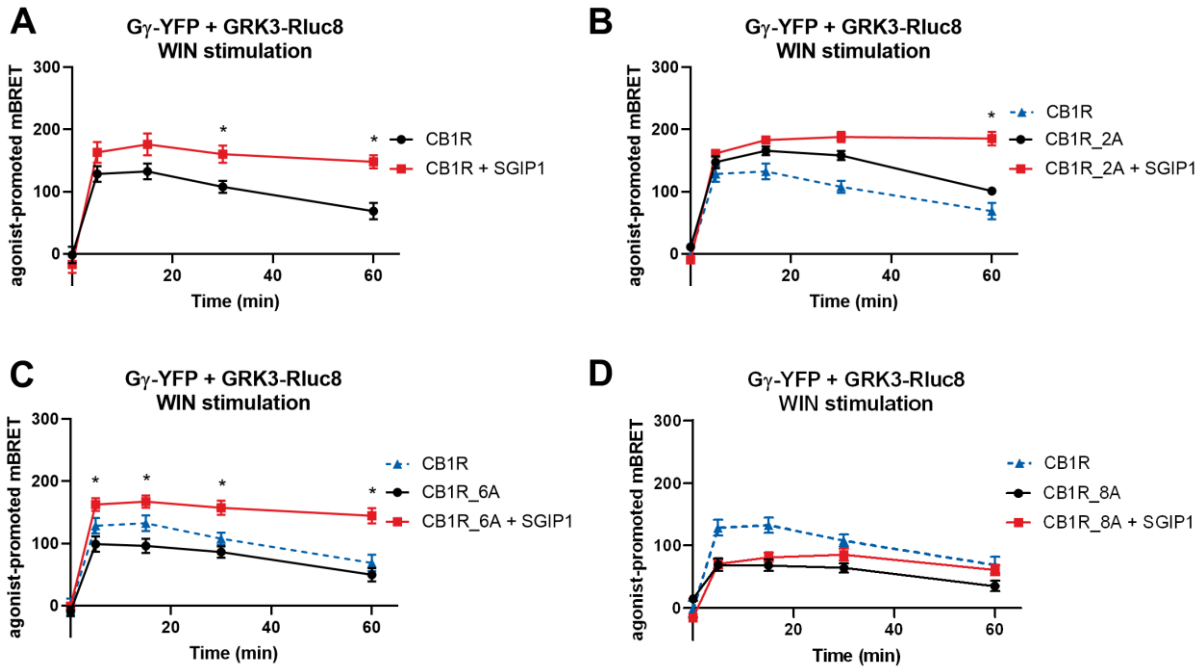

Fig. 3. Formation of GRK3-Gβγ complexes is partially independent of CB1R C-tail phosphorylation. SGIP1 enhances the association GRK3-Gβγ complexes in the mutant receptors that interact with partner proteins. *HEK293 were transiently co-transfected with CB1R, GRK3-Rluc8, Gγ-YFP, Gβ, and empty vector/SGIP1-mCherry (1:1:2:1:2 ratio). 24 hours after transfection, cells were stimulated by 1 μM WIN.* ***A)*** *Kinetic profile of GRK3 recruitment to Gγ in CB1R, in the presence and absence of SGIP1.* ***B)*** *Kinetic profile of GRK3 recruitment to Gγ in CB1R, CB1R_2A and CB1R_2A + SGIP1.* ***C)*** *Kinetic profile of GRK3 recruitment to Gγ driven by CB1R and CB1R_6A in presence/absence of SGIP1.* ***D)*** *Kinetic profile of GRK3 recruitment to Gγ driven by CB1R and CB1R_8A in presence/absence of SGIP1. Data represent the mean ± SEM of three expriments of independent cell preparations performed in 3 technical replicates. * represents $p \leq 0.05$ (full statistical analysis is disclosed in Table 2 and Table 3).*

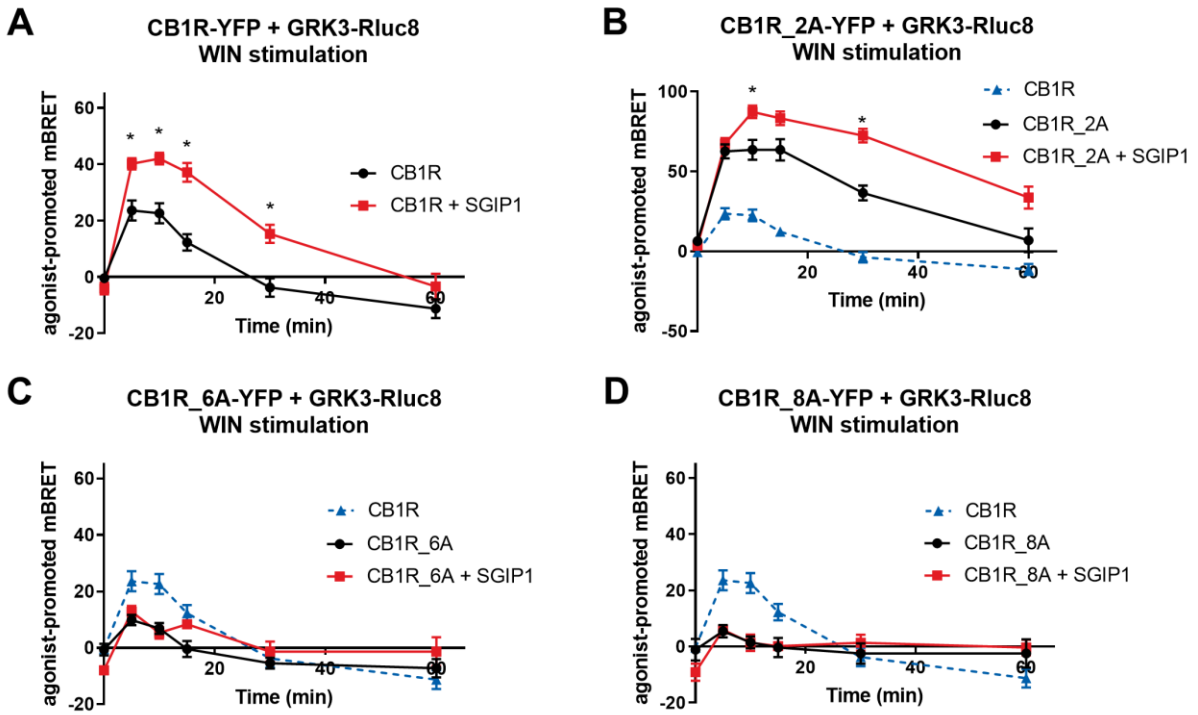

Fig. 4. C-tail multisite phosphorylation is crucial for GRK3 recruitment and dissociation. SGIP1 enhances association of CB1R-GRK3 in CB1R mutants that interact with GRK3. *HEK293 cells were transiently co-transfected with the plasmids coding CB1R-YFP variant + GRK3-RLuc8 + empty plasmid pRK6/SGIP1-mCherry (2:1:2 ratio). Cells were stimulated by WIN55212-2 (WIN, 1 µM).* ***A)*** *Kinetic profile of GRK3 recruitment to CB1R in the presence and absence of SGIP1.* ***B)*** *Kinetic profile of GRK3 recruitment to CB1R, CB1R_2A and CB1R_2A + SGIP1.* ***C)*** *Kinetic profile of GRK3 recruitment to CB1R and CB1R_6A in the presence or absence of SGIP1.* ***D)*** *Kinetic profile of GRK3 recruitment to CB1R, CB1R_8A and CB1R_8A + SGIP1. Data represent the mean ± SEM of three expriments of independent cell preparations performed in 3 technical replicates. * represents p ≤ 0.05 (full statistical analysis is disclosed in Table 4 and 5).*

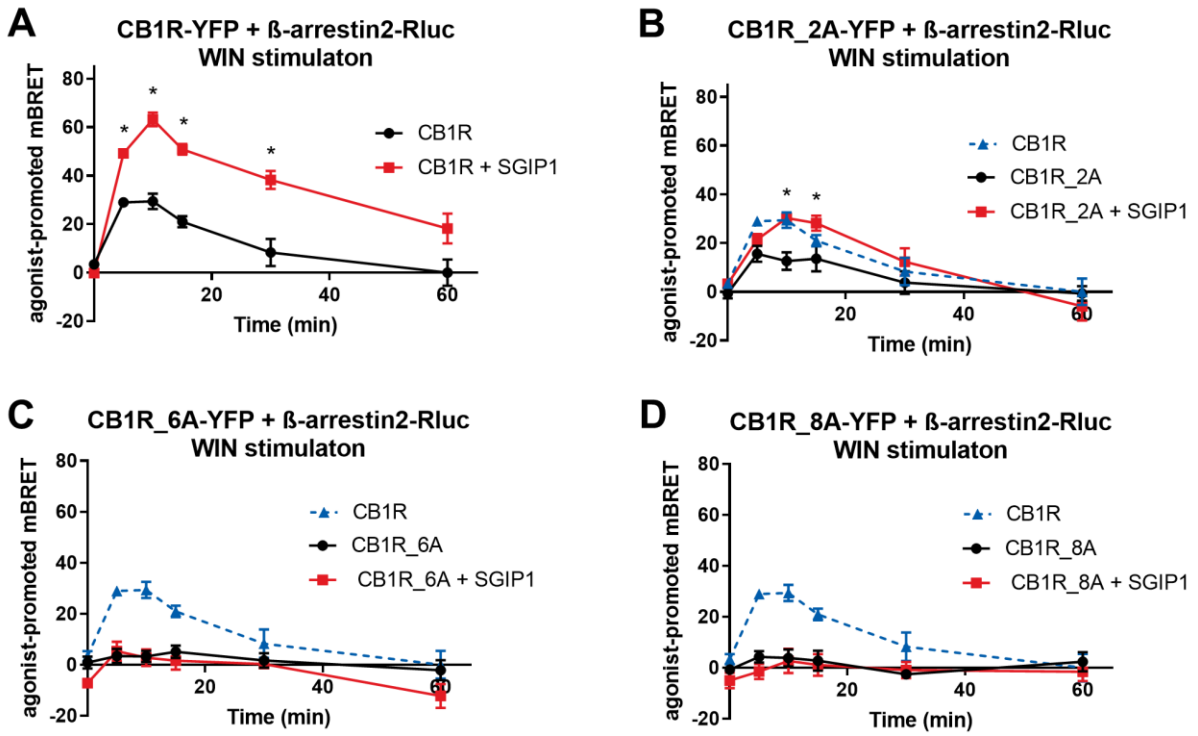

Fig. 5. β-arrestin2 binding is affected by the phosphorylation pattern of the CB1R C-tail. SGIP1 enhances the association of CB1R-β-arrestin2 in the mutant receptors that interact with β-arrestin2. *HEK293 cells were transiently co-transfected with the CB1R-YFP variants, β-arrestin2-Rluc, and empty vector/SGIP1-mCherry (2:1:2 ratio). Cells were stimulated by 1 µM WIN.* ***A)*** *Kinetic profile of β-arrestin2 recruitment to CB1R in the presence/absence of SGIP1.* ***B)*** *Kinetic profile of β-arrestin2 recruitment to CB1R, CB1R_2A and CB1R_2A + SGIP1.* ***C)*** *Kinetic profile of β-arrestin2 recruitment to CB1R and CB1R_6A in the presence/absence of SGIP1.* ***D)*** *Kinetic profile of β-arrestin2 recruitment to CB1R, CB1R_8A and CB1R_8A + SGIP1. Data represent the mean ± SEM from 3 expriments of independent cell preparations performed in triplicate. * represents $p \leq 0.05$ (full statistical analysis is disclosed in Table 6 and 7).*

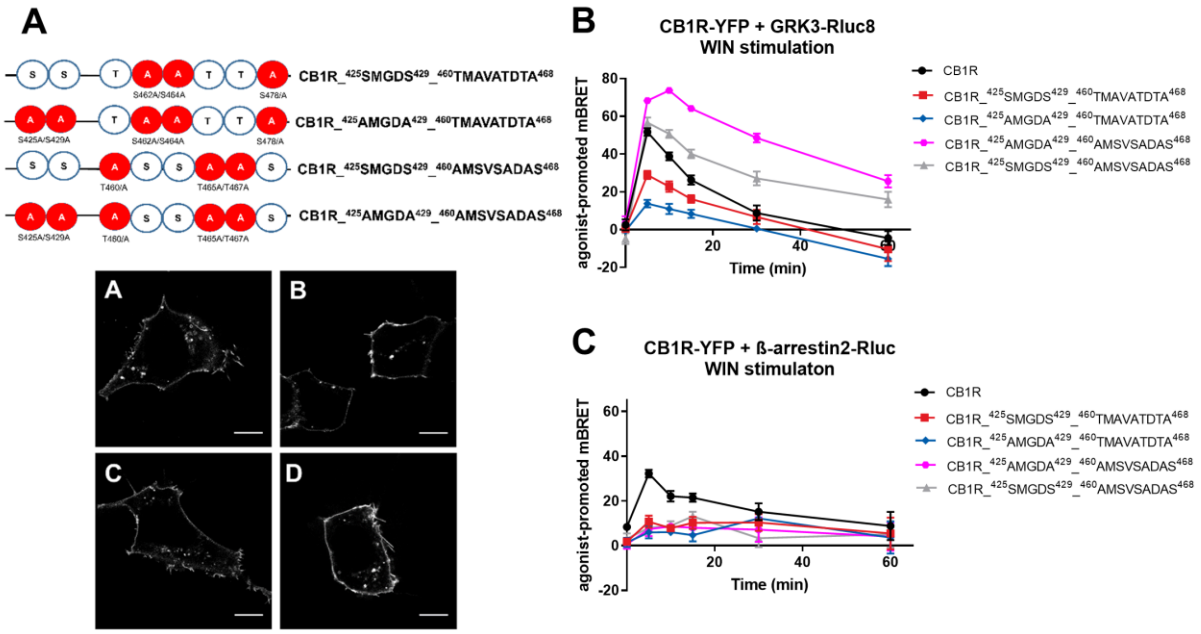

Fig. 6. GRK3 and ß-arrestin2 interactions with CB1R depend on unique phosphorylation patterns. ***A)*** *Schematic depiction of constructed CB1R mutants and their cellular localization. A - mutation into alanine. HEK293 cells were transiently transfected with CB1R-YFP variant. 24 hours after transfection, cells were visualized using fluorescent microscope. A) CB1R_*^{456}*SMGDS*^{429}*_*^{460}*TMAVATDTA*^{468}*, B) CB1R_*^{456}*AMGDA*^{429}*_*^{460}*TMAVATDTA*^{468}*, C) CB1R_*^{456}*SMGDS*^{429}*_*^{460}*AMSVSADAS*^{468}*, D) CB1R_*^{456}*AMGDA*^{429}*_*^{460}*AMSVSADAS*^{468}*. Scale bar represents 10 µm.* ***B)*** *Kinetic profile of GRK3 recruitment to CB1R and CB1R mutants.* ***C)*** *Kinetic profile of ß-arrestin2 recruitment to CB1R and CB1R mutants. Data represent the mean ± SEM from 3 independent cell preparations experiments performed in triplicate.*

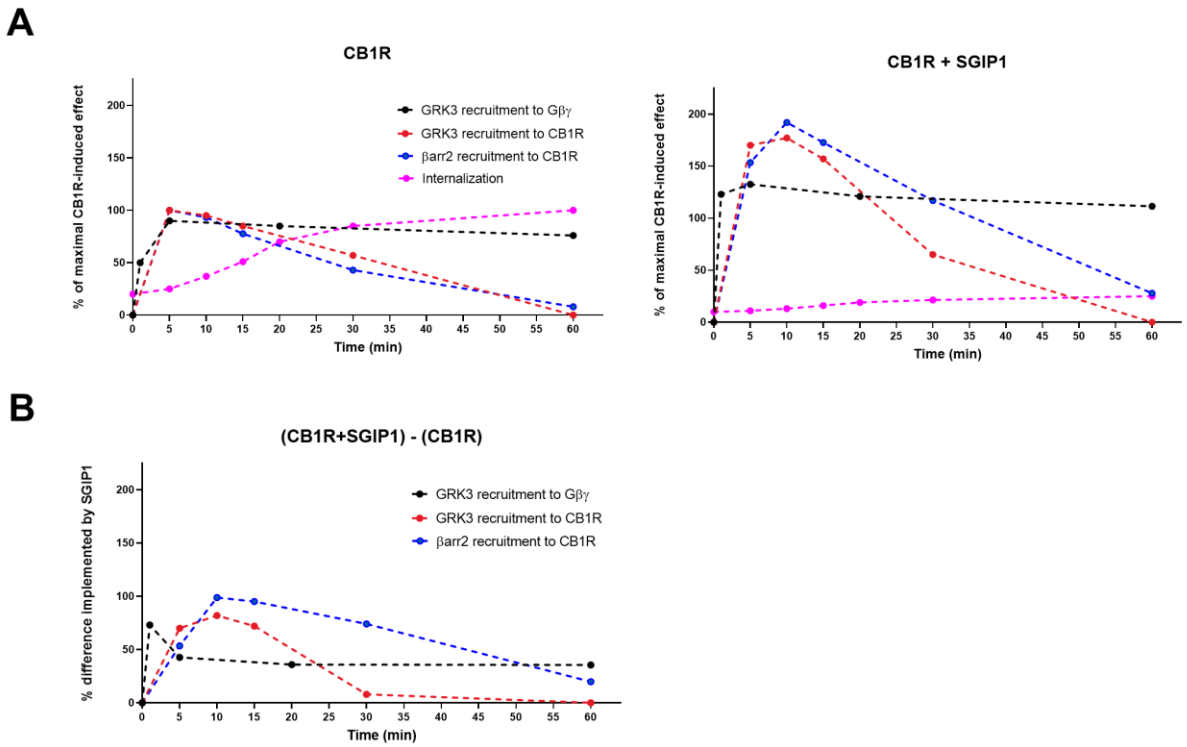

Fig. 7. Graphic depiction of events relevant to CB1R desensitization. ***A)*** *Kinetics of events during desensitization of CB1R in the absence (left panel) and the presence (right panel) of SGIP1 upon CB1R stimulation with 1 μM WIN in HEK293 cells.* ***B)*** *The difference in interactions implemented by SGIP1. Values were calculated by subtracting the kinetics values of CB1R + SGIP1 with the values of CB1R. Figure was constructed using calculated data from the experimets. Curves of Barr2 and GRK3 recruitment to CB1R as well as GRK3 binding to Gβγ were calculated from the presented study, curve of CB1R internalization was calculated from previous study*

SGIP1 modulates kinetics and interactions of the cannabinoid receptor 1 and G protein-coupled receptor kinase 3 signalosome

Supplementary material

Matej Gazdarica[1, 2], Judith Noda[1], Oleh Durydivka[1], Vendula Novosadova[3], Ken Mackie[4], Jean-Philippe Pin[2], Laurent Prezeau[2, 5], Jaroslav Blahos[1, 5]

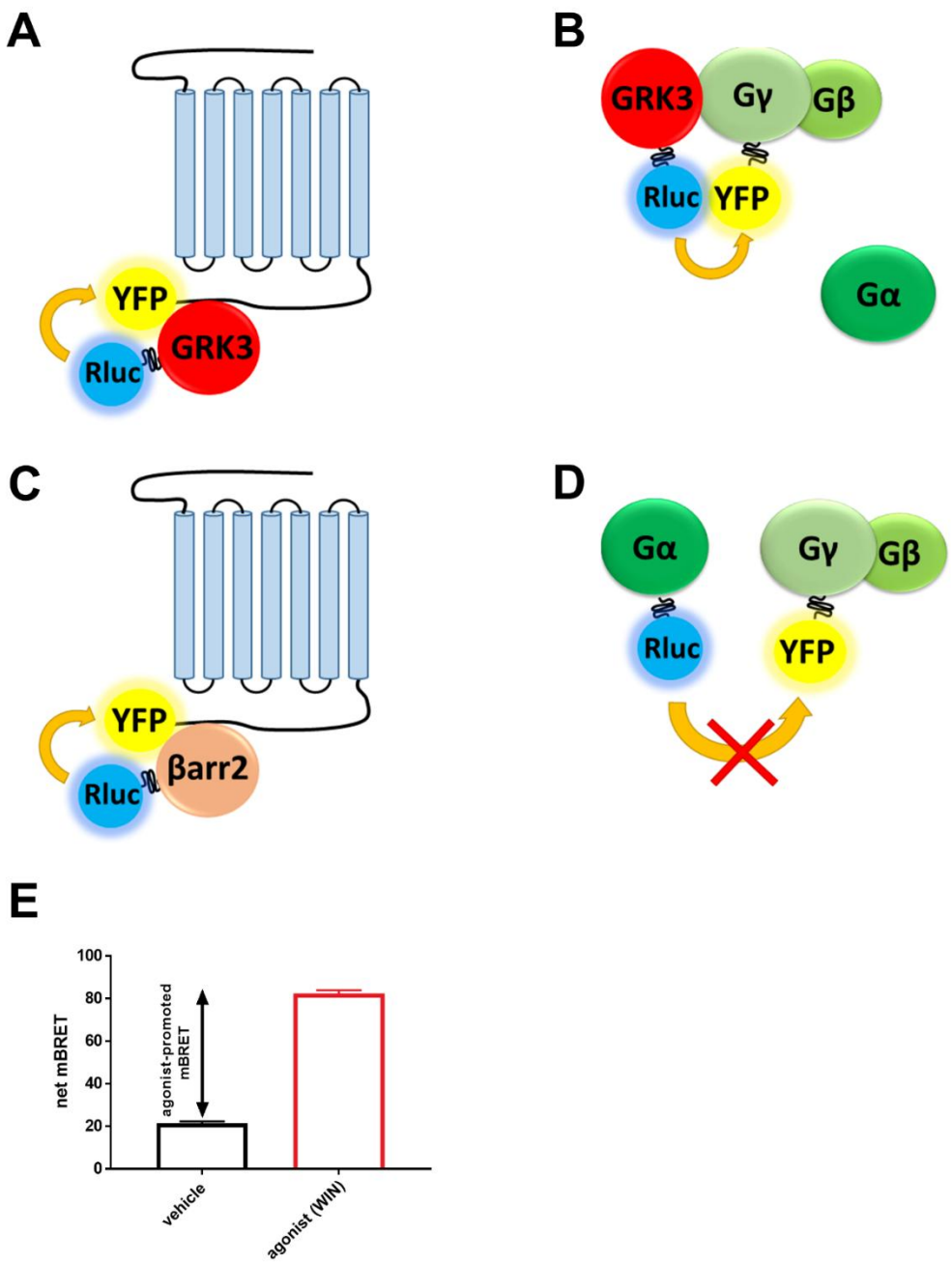

Suppl. Fig. 1. BRET based sensors used in the study. ***A)*** *Schematic representation of GRK3-RLuc8 recruitment to CB1R-YFP upon CB1R activation. The formation of GRK3-CB1R complexes is observed as an increase in BRET signal efficiency.* ***B)*** *Schematic representation of GRK3-Rluc8 with Gγ-YFP complexes formation generating an increase of BRET signal.* ***C)*** *Schematic representation of the recruitment of β-arrestin2-Rluc by the activated CB1R-YFP generating an increase of BRET signal.* ***D)*** *Schematic representation of the activation of heterotrimeric G proteins which is observed as a decrease in BRET signal due to dissociation/conformational change of $G\alpha_i$ from Gβγ subunits.* ***E)*** *Agonist-promoted mBRET was calculated by subtracting the BRET ratio obtained in the absence of agonist from the one obtained following agonist application and multiplied by 1000.*

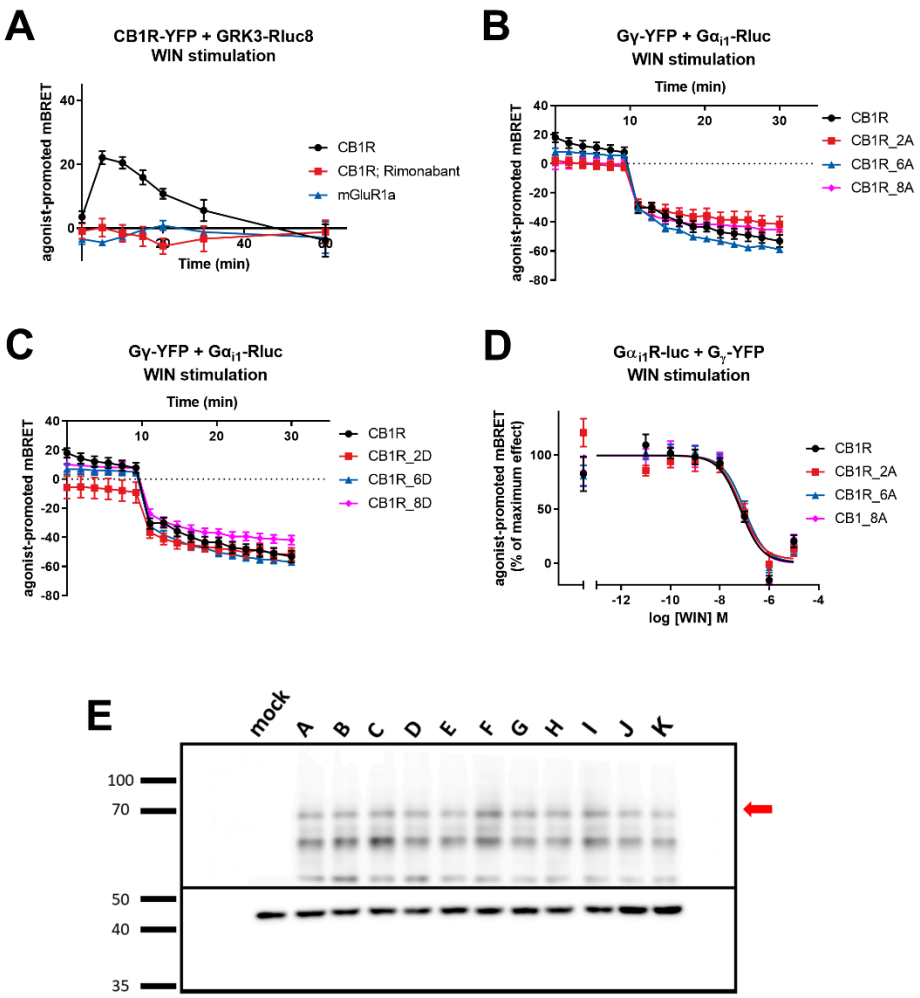

Suppl. Fig. 2. GRK3 recruitment by WIN-activated. CB1R Multisite phosphorylation CB1R mutants retain the capability to induce rapid dissociation of G protein subunits. Mutant CB1Rs variants have similar levels of expression to wild-type CB1R. ***A)*** *Kinetic profiles of GRK3-RLuc8 recruitment by WIN-activated CB1R-YFP/mGluR1a in HEK293 cells pretreated or not with rimonabant. HEK293 cells were transiently cotransfected with the plasmid coding for CB1R-YFP or mGluR1a and GRK3-RLuc8. After sixteen hours, cells were pretreated or not for 30 minutes with rimonabant (45 μM) prior to the stimulation with the CB1R agonist WIN (1 μM).* ***B)*** *Alanine mutant CB1Rs preserve the ability to activate of G proteins. HEK293 cells were transiently cotransfected with CB1R-SNAP variant, Gα$_i$-Rluc8, Gβ-Flag, Gγ-YFP (2:1:1:1 ratio). Firstly, basal BRET was measured for 10 minutes. Afterward, cells were stimulated by 1 μM WIN.* ***C)*** *Aspartic acid mutant CB1Rs preserve the ability to activate of G proteins. HEK293 cells were transiently cotransfected with CB1R-SNAP variant, Gα$_i$-Rluc8, Gβ-Flag, Gγ-YFP (2:1:1:1 ratio). Firstly, basal BRET was measured for 10 minutes. Afterward, cells were stimulated by 1 μM WIN.* ***D)*** *C-tail mutations do not significantly change acute CB1R mediated Gα$_i$ protein activation. Dose-response curves of Gα$_i$ subunit dissociation from the Gγ-YFP after CB1R stimulation with increasing concentrations of WIN. HEK293 cells were transiently cotransfected with CB1R-SNAP variant, Gα$_i$-Rluc8, Gβ-Flag, Gγ-YFP (2:1:1:1 ratio). Twenty-four hours after transfection, 5 μM coelenterazine h was added, cells were stimulated with increasing concentrations of WIN and the decrease in BRET signal was measured 15 minutes after WIN application.* ***E)*** *Mutant CB1Rs variants have similar levels of expression to wild-type CB1R. HEK293 cells were transfected with the indicated CB1R variant or with empty plasmid pRK6 (mock). Cell lysates were separated by SDS-PAGE and subjected to Western blotting. Membranes were stained with either anti-GFP antibody for*

detection of CB1R-YFP variants (top blot) or anti-Actin antibody (actin) to normalize for loading and transfer of proteins (bottom blot). Legend: mock (pRK6 empty vector transfection), A) CB1R, B) CB1R_2A, C) CB1R_6A, D) CB1R_8A, E) CB1R_2D, F) CB1R_6D, G) CB1R_8D, H) CB1R_^{456}SMGDS^{429}_^{460}TMAVATDTA^{468}, I) CB1R_^{456}AMGDA^{429}_^{460}TMAVATDTA^{468}, J) CB1R_^{456}SMGDS^{429}_^{460}AMSVSADAS^{468}, K) CB1R_^{456}AMGDA^{429}_^{460}AMSVSADAS^{468}.

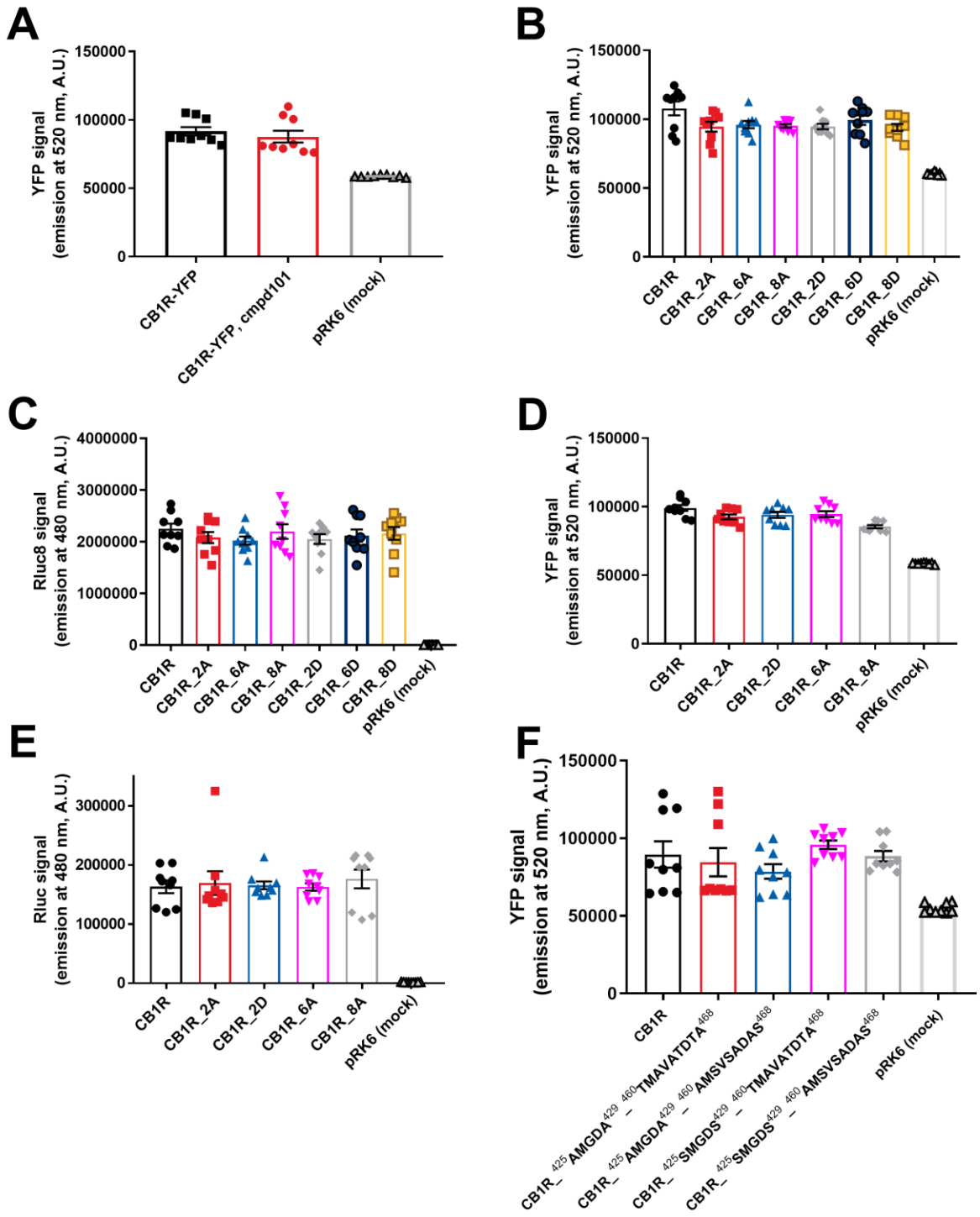

Suppl. Fig. 3. Expression levels of CB1R-YFP variants, GRK3-Rluc8 and β-arrestin2-Rluc in transiently transfected HEK293 cells. *Emission of CB1R-YFP variants was measured at 520 nm on Mithras LB 940 microplate reader. Emission of Rluc constructs was measured at 480 nm on Mithras LB 940 microplate reader 5 minutes after adding coelenterazine h.* ***A)*** *Cmpd101 does not affect the expression of CB1R-YFP. Expression level determination of CB1R-YFP in presence/absence of cmpd101.* ***B)*** *Expression levels of CB1R-YFP variants.* ***C)*** *GRK3-Rluc8 in cells coexpressing mutant CB1Rs.* ***D)*** *Expression levels of CB1R-YFP variants.* ***E)*** *β-arrestin2-Rluc in cells coexpressing mutant CB1R.* ***F)*** *Expression level determination of CB1R-YFP variants.*

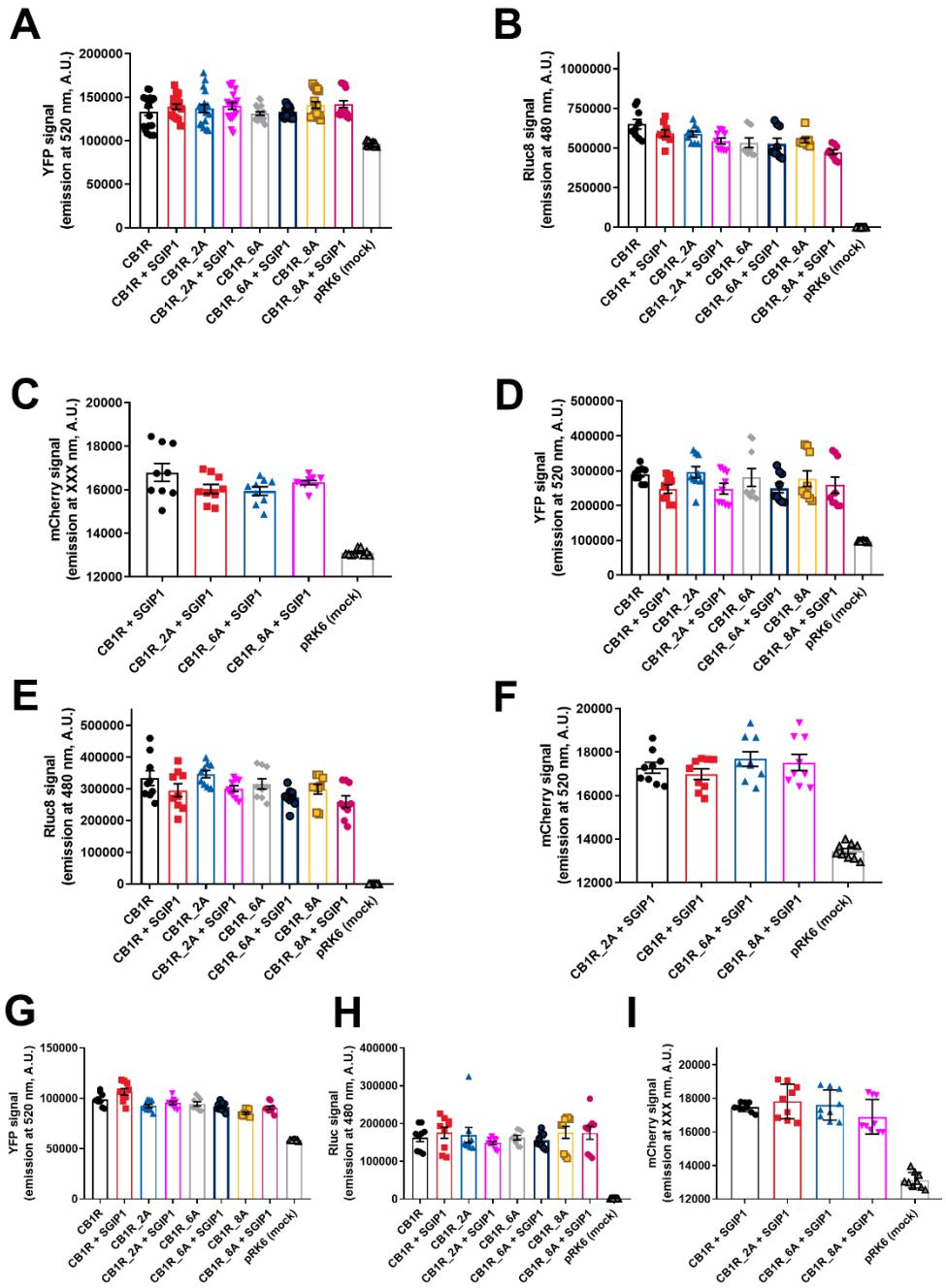

Suppl. Fig. 4. Expression level determination of CB1R-YFP variants, GRK3-Rluc8, β-arrestin2-Rluc and SGIP1-mCherry in transiently transfected HEK293 cells. *Emission of YFP proteins was measured at 520 nm on Mithras LB 940 microplate reader. Emission of Rluc constructs was measured at 480 nm on Mithras LB 940 microplate reader 5 minutes after adding coelenterazine h. Emission of SGIP1-mCherry was measured at 600 nm on Mithras LB 940 microplate.* ***A)*** *Expression level determination of CB1R-YFP variants in cells coexpressing SGIP1-mCherry and GRK3-Rluc8.* ***B)*** *GRK3-Rluc8 in cells coexpressing mutant CB1Rs.* ***C)*** *SGIP1-mCherry expression in cells coexpressing different CB1R receptors.* ***D)*** *Expression level determination of CB1R-YFP variants in cells coexpressing SGIP1-mCherry and β-arrestin2-Rluc.* ***E)*** *β-arrestin2-Rluc in cells coexpressing mutant CB1Rs.* ***F)*** *SGIP1-mCherry expression in cells coexpressing different CB1R receptors.* ***G)*** *Expression level determination of Gγ-YFP cells coexpressing distinct CB1R-SNAP variant, SGIP1-mCherry and GRK3-Rluc8.* ***H)*** *GRK3-Rluc8 in cells coexpressing mutant CB1R-SNAP.* ***I)*** *SGIP1-mCherry expression in cells coexpressing different CB1R receptors.*

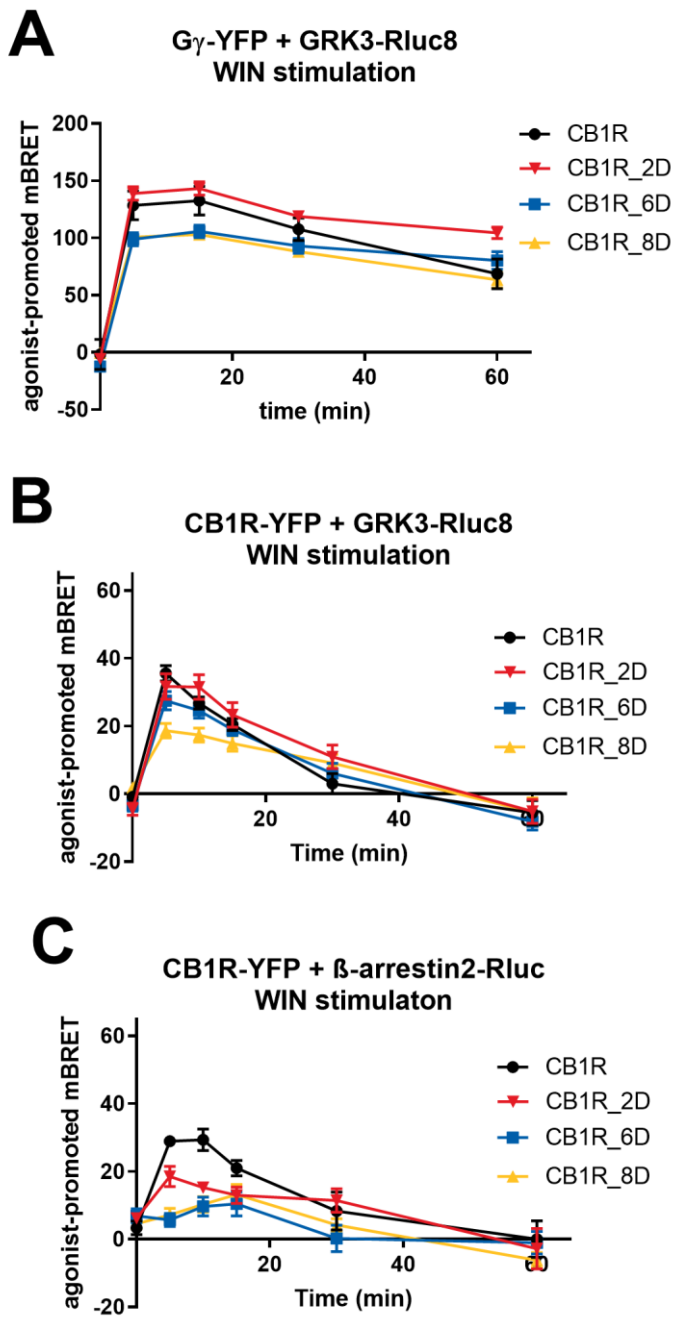

Suppl. Fig. 5. Protein-protein interactions driven by aspartic acid CB1R mutants. *HEK293 were transiently co-transfected with either CB1R-YFP variant, GRK3-Rluc8 and empty plasmid pRK6 or CB1R_YFP variant, ß-arrestin2-Rluc and empty plasmid pRK6 or CB1R-SNAP, GRK3-Rluc8, Gγ-YFP, Gß, and empty vector pRK6 (1:1:2:1:2 ratio). 24 hours after the transfection, cells were stimulated by 1 µM WIN.* ***A)*** *Kinetics of GRK3 recruitment to Gγ driven by CB1R, CB1R_2D, CB1R_6D, CB1R_8D.* ***B)*** *Kinetics of GRK3 recruitment to CB1R, CB1R_2D, CB1R_6D, CB1R_8D.* ***C)*** *Kinetics of ß-arrestin2 recruitment to CB1R, CB1R_2D, CB1R_6D, CB1R_8D.*

A

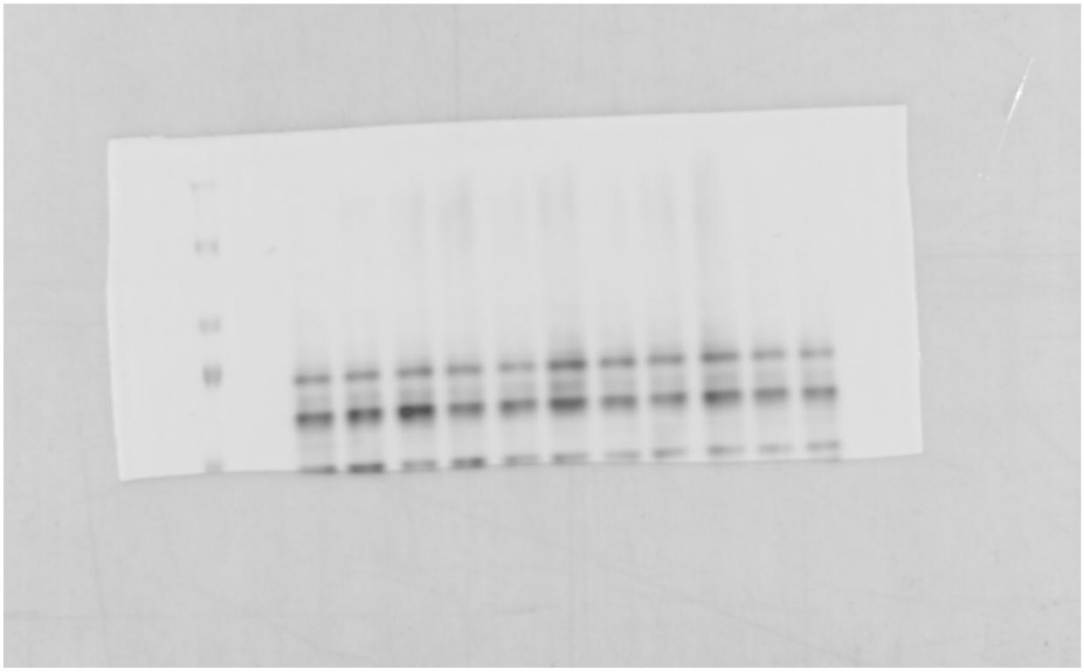

B

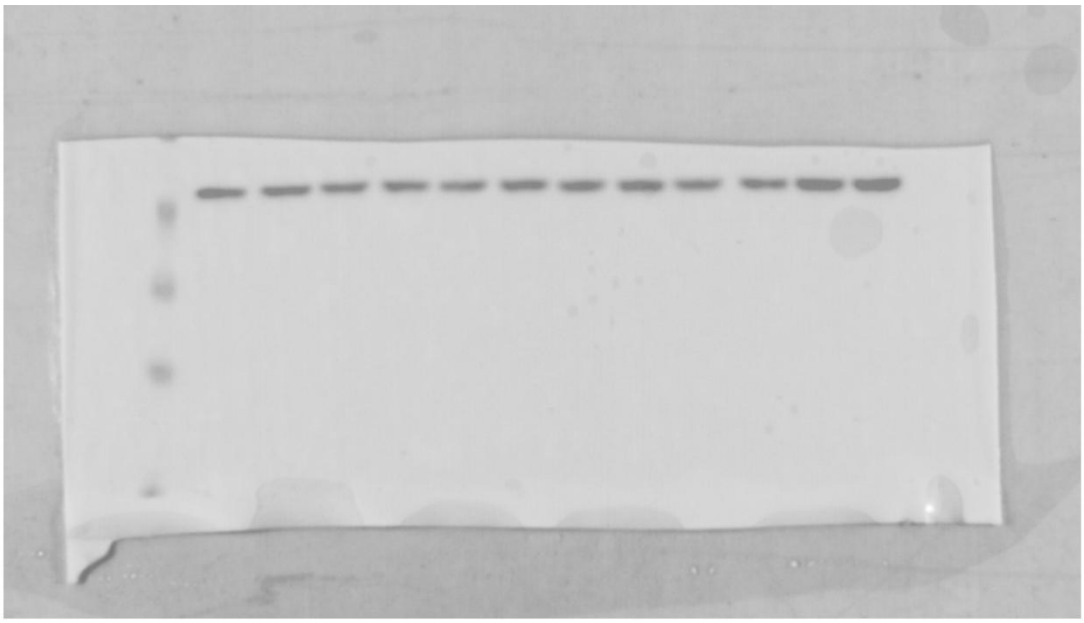

Suppl. Fig. 6. Full uncropped western blot image from Supp. Fig. 2E.

A

Gγ-YFP + GRK3-Rluc8 +- cmpd101

ANOVA table	SS	DF	MS	F (DFn, DFd)	P value
Time x cmpd101 treatment	30198	4	7550	F (4, 40) = 58.33	P<0.0001
Time	154175	4	38544	F (4, 40) = 85.88	P<0.0001
cmpd101 treatment	145702	1	145702	F (1, 40) = 1126	P<0.0001

Šídák's multiple comparisons test	Mean Diff.	95.00% CI of diff.	Below threshold?	Summary	Adjusted P Value
CB1R vs CB1R + cmpd101					
0 min	9.834	-4.627 to 24.30	No	ns	0.3197
5 min after WIN stimulation	103.0	88.50 to 117.4	Yes	****	<0.0001
15 min after WIN stimulation	112.0	97.50 to 126.4	Yes	****	<0.0001
30 min after WIN stimulation	95.31	80.85 to 109.8	Yes	****	<0.0001
60 min after WIN stimulation	82.29	67.83 to 96.75	Yes	****	<0.0001

B

CB1R-YFP + GRK3-Rluc8 +- cmpd101

ANOVA table	SS	DF	MS	F (DFn, DFd)	P value
Time x cmpd101 treatment	1213	5	242.5	F (5, 80) = 19.57	P<0.0001
Time	5161	5	1032	F (2.043, 32.69) = 83.29	P<0.0001
cmpd101 treatment	2480	1	2480	F (1, 16) = 23.54	P=0.0002

Šídák's multiple comparisons test	Mean Diff.	95.00% CI of diff.	Below threshold?	Summary	Adjusted P Value
CB1R vs CB1R + cmpd101					
0 min	0.5299	-6.814 to 7.874	No	ns	>0.9999
5 min after WIN stimulation	18.58	11.56 to 25.59	Yes	****	<0.0001
10 min after WIN stimulation	16.43	8.811 to 24.04	Yes	****	<0.0001
15 min after WIN stimulation	12.65	6.149 to 19.16	Yes	***	0.0002
30 min after WIN stimulation	3.689	-3.301 to 10.68	No	ns	0.5737
60 min after WIN stimulation	5.629	-3.573 to 14.83	No	ns	0.4104

C

CB1R-YFP + ß-arrestin2-Rluc +- cmpd101

ANOVA table	SS	DF	MS	F (DFn, DFd)	P value
Time x cmpd101 treatment	3681	5	736.1	F (5, 80) = 16.98	P<0.0001
Time	3436	5	687.2	F (5, 80) = 15.85	P<0.0001
cmpd101 treatment	4368	1	4368	F (1, 16) = 35.04	P<0.0001

Šídák's multiple comparisons test	Mean Diff.	95.00% CI of diff.	Below threshold?	Summary	Adjusted P Value
CB1R vs CB1R + cmpd101					
0 min	-1.184	-7.590 to 5.223	No	ns	0.9946
5 min after WIN stimulation	28.70	16.21 to 41.20	Yes	****	<0.0001
10 min after WIN stimulation	24.25	11.42 to 37.07	Yes	***	0.0003
15 min after WIN stimulation	18.10	5.596 to 30.61	Yes	**	0.0031
30 min after WIN stimulation	6.890	-2.177 to 15.96	No	ns	0.2007
60 min after WIN stimulation	-0.4430	-11.34 to 10.46	No	ns	>0.9999

Table 1. Statistical analysis of kinetics of presented protein-protein interactions. *Curves were compared by two-way ANOVA followed by Sidak's multiple comparison test. If the curves were significantly different, post hoc analysis of time points was performed.*

Gγ-YFP + GRK3-Rluc8 – CB1R, CB1R_2A, CB1R_6A, CB1R_8A

ANOVA table	SS	DF	MS	F (DFn, DFd)	P value
Time x CB1R variant	35899	12	2992	F (12, 128) = 7.938	P<0.0001
Time	319548	4	79887	F (1.627, 52.06) = 212.0	P<0.0001
CB1R variant	113790	3	37930	F (3, 32) = 13.53	P<0.0001

Šídák's multiple comparisons test	Mean Diff.	95.00% CI of diff.	Below threshold?	Summary	Adjusted P Value
0 min					
CB1R vs. CB1R_2A	-12.77	-65.76 to 40.23	No	ns	0.9993
CB1R vs. CB1R_6A	7.168	-47.44 to 61.78	No	ns	>0.9999
CB1R vs. CB1R_8A	-16.29	-69.39 to 36.81	No	ns	0.9925
5 min after WIN stimulation					
CB1R vs. CB1R_2A	-18.82	-74.00 to 36.36	No	ns	0.9878
CB1R vs. CB1R_6A	29.46	-31.48 to 90.40	No	ns	0.8438
CB1R vs. CB1R_8A	59.70	3.323 to 116.1	Yes	*	0.0330
15 min after WIN stimulation					
CB1R vs. CB1R_2A	-33.03	-85.00 to 18.95	No	ns	0.4629
CB1R vs. CB1R_6A	36.71	-22.02 to 95.44	No	ns	0.5177
CB1R vs. CB1R_8A	64.44	10.25 to 118.6	Yes	*	0.0135
30 min after WIN stimulation					
CB1R vs. CB1R_2A	-50.33	-93.09 to -7.561	Yes	*	0.0145
CB1R vs. CB1R_6A	21.47	-24.16 to 67.09	No	ns	0.8665
CB1R vs. CB1R_8A	43.76	1.341 to 86.17	Yes	*	0.0401
60 min after WIN stimulation					
CB1R vs. CB1R_2A	-32.50	-85.49 to 20.48	No	ns	0.4907
CB1R vs. CB1R_6A	18.94	-39.45 to 77.32	No	ns	0.9927
CB1R vs. CB1R_8A	33.50	-21.05 to 88.05	No	ns	0.5199

Table 2. Statistical analysis of kinetics of presented protein-protein interactions. *Curves were compared by two-way ANOVA followed by Sidak's multiple comparison test. If the curves were significantly different, post hoc analysis of time points was performed.*

A **Gγ-YFP + GRK3-Rluc8 – CB1R +- SGIP1**

ANOVA table	SS	DF	MS	F (DFn, DFd)	P value
Time x +- SGIP1	37097	5	7419	F (5, 80) = 13.81	P<0.0001
Time	533999	5	106800	F (1.427, 22.83) = 198.8	P<0.0001
+- SGIP1	21381	1	21381	F (1, 16) = 2.940	P=0.1057

Šídák's multiple comparisons test	Mean Diff.	95.00% CI of diff.	Below threshold?	Summary	Adjusted P Value
CB1R vs CB1R + SGIP1					
0 min	15.55	-40.96 to 72.05	No	ns	0.9625
5 min after WIN stimulation	-34.67	-98.43 to 29.08	No	ns	0.5364
15 min after WIN stimulation	-43.23	-108.7 to 22.22	No	ns	0.3258
30 min after WIN stimulation	-52.62	-104.4 to -0.8715	Yes	*	0.0452
60 min after WIN stimulation	-79.20	-130.1 to -28.31	Yes	**	0.0016

B **Gγ-YFP + GRK3-Rluc8 – CB1R_2A +- SGIP1**

ANOVA table	SS	DF	MS	F (DFn, DFd)	P value
Time x +- SGIP1	37906	5	7581	F (5, 80) = 30.30	P<0.0001
Time	632583	5	126517	F (2.341, 37.46) = 505.7	P<0.0001
+- SGIP1	6581	1	6581	F (1, 16) = 4.507	P=0.0497

Šídák's multiple comparisons test	Mean Diff.	95.00% CI of diff.	Below threshold?	Summary	Adjusted P Value
CB1R_2A vs CB1R_2A + SGIP1					
0 min	20.60	-1.657 to 42.85	No	ns	0.0785
5 min after WIN stimulation	-14.09	-49.76 to 21.58	No	ns	0.8176
15 min after WIN stimulation	-17.28	-45.26 to 10.69	No	ns	0.4000
30 min after WIN stimulation	-29.85	-63.24 to 3.547	No	ns	0.0946
60 min after WIN stimulation	-84.26	-122.6 to -45.93	Yes	****	<0.0001

C **Gγ-YFP + GRK3-Rluc8 – CB1R_6A +- SGIP1**

ANOVA table	SS	DF	MS	F (DFn, DFd)	P value
Time x +- SGIP1	32253	5	6451	F (5, 80) = 21.12	P<0.0001
Time	387015	5	77403	F (1.798, 28.77) = 253.5	P<0.0001
+- SGIP1	72338	1	72338	F (1, 16) = 20.37	P=0.0004

Šídák's multiple comparisons test	Mean Diff.	95.00% CI of diff.	Below threshold?	Summary	Adjusted P Value
CB1R_6A vs CB1R_6A + SGIP1					
0 min	-8.203	-36.64 to 20.24	No	ns	0.9439
5 min after WIN stimulation	-63.58	-112.6 to -14.60	Yes	**	0.0079
15 min after WIN stimulation	-71.15	-117.3 to -25.02	Yes	**	0.0017
30 min after WIN stimulation	-71.14	-115.6 to -26.69	Yes	**	0.0013
60 min after WIN stimulation	-94.90	-144.0 to -45.85	Yes	***	0.0002

D **Gγ-YFP + GRK3-Rluc8 – CB1R_8A +- SGIP1**

ANOVA table	SS	DF	MS	F (DFn, DFd)	P value
Time x +- SGIP1	13219	5	2644	F (5, 80) = 10.65	P<0.0001
Time	124357	5	24871	F (2.275, 36.40) = 100.2	P<0.0001
+- SGIP1	8.017	1	8.017	F (1, 16) = 0.004352	P=0.9482

Table 3. Statistical analysis of kinetics of presented protein-protein interactions. *Curves were compared by two-way ANOVA followed by Sidak's multiple comparison test. If the curves were significantly different, post hoc analysis of time points was performed.*

CB1R-YFP + GRK3-Rluc8 – CB1R, CB1R_2A, CB1R_6A, CB1R_8A

ANOVA table	SS	DF	MS	F (DFn, DFd)	P value
Time x CB1R variant	19456	15	1297	F (15, 160) = 17.41	P<0.0001
Time	27135	5	5427	F (3.012, 96.40) = 72.84	P<0.0001
CB1R variant	58182	3	19394	F (3, 32) = 46.48	P<0.0001

Šídák's multiple comparisons test	Mean Diff.	95.00% CI of diff.	Below threshold?	Summary	Adjusted P Value
0 min					
CB1R vs. CB1R_2A	-6.820	-13.87 to 0.2316	No	ns	0.0588
CB1R vs. CB1R_6A	0.1555	-6.227 to 6.538	No	ns	0.9999
CB1R vs. CB1R_8A	0.7040	-10.93 to 12.34	No	ns	0.9975
5 min after WIN stimulation					
CB1R vs. CB1R_2A	-38.91	-54.16 to -23.66	Yes	****	<0.0001
CB1R vs. CB1R_6A	13.73	2.633 to 24.83	Yes	*	0.0148
CB1R vs. CB1R_8A	18.17	6.791 to 29.56	Yes	**	0.0022
10 min after WIN stimulation					
CB1R vs. CB1R_2A	-40.99	-60.87 to -21.12	Yes	***	0.0003
CB1R vs. CB1R_6A	15.66	4.394 to 26.93	Yes	**	0.0068
CB1R vs. CB1R_8A	21.06	9.619 to 32.50	Yes	***	0.0007
15 min after WIN stimulation					
CB1R vs. CB1R_2A	-51.33	-71.93 to -30.72	Yes	****	<0.0001
CB1R vs. CB1R_6A	12.71	1.939 to 23.48	Yes	*	0.0187
CB1R vs. CB1R_8A	12.62	0.5938 to 24.64	Yes	*	0.0384
30 min after WIN stimulation					
CB1R vs. CB1R_2A	-40.31	-55.68 to -24.95	Yes	****	<0.0001
CB1R vs. CB1R_6A	1.751	-8.621 to 12.12	No	ns	0.9576
CB1R vs. CB1R_8A	-1.273	-14.38 to 11.83	No	ns	0.9919
60 min after WIN stimulation					
CB1R vs. CB1R_2A	-18.20	-40.74 to 4.351	No	ns	0.1280
CB1R vs. CB1R_6A	-4.015	-16.58 to 8.551	No	ns	0.7916
CB1R vs. CB1R_8A	-8.775	-25.21 to 7.664	No	ns	0.4283

Table 4. Statistical analysis of kinetics of presented protein-protein interactions. *Curves were compared by two-way ANOVA followed by Sidak's multiple comparison test. If the curves were significantly different, post hoc analysis of time points was performed.*

A **CB1R-YFP + GRK3-Rluc8 +- SGIP1**

ANOVA table	SS	DF	MS	F (DFn, DFd)	P value
Time x +- SGIP1	2379	5	475.8	F (5, 80) = 7.613	P<0.0001
Time	28003	5	5601	F (2.339, 37.42) = 89.61	P<0.0001
+- SGIP1	5295	1	5295	F (1, 16) = 28.23	P<0.0001

Šídák's multiple comparisons test	Mean Diff.	95.00% CI of diff.	Below threshold?	Summary	Adjusted P Value
CB1R vs CB1R + SGIP1					
0 min	3.686	-3.527 to 10.90	No	ns	0.5737
5 min after WIN stimulation	-16.55	-29.22 to -3.871	Yes	**	0.0085
10 min after WIN stimulation	-19.44	-32.26 to -6.621	Yes	**	0.0026
15 min after WIN stimulation	-24.81	-38.13 to -11.50	Yes	***	0.0003
30 min after WIN stimulation	-19.03	-32.69 to -5.373	Yes	**	0.0043
60 min after WIN stimulation	-7.876	-25.03 to 9.275	No	ns	0.7054

B **CB1R_2A-YFP + GRK3-Rluc8 +- SGIP1**

ANOVA table	SS	DF	MS	F (DFn, DFd)	P value
Time x +- SGIP1	4649	5	929.8	F (5, 80) = 6.885	P<0.0001
Time	78239	5	15648	F (2.298, 36.77) = 115.9	P<0.0001
+- SGIP1	8754	1	8754	F (1, 16) = 12.67	P=0.0026

Šídák's multiple comparisons test	Mean Diff.	95.00% CI of diff.	Below threshold?	Summary	Adjusted P Value
CB1R_8A vs CB1R_8A + SGIP1					
0 min	2.844	-7.480 to 13.17	No	ns	>0.9999
5 min after WIN stimulation	-4.964	-22.11 to 12.19	No	ns	>0.9999
10 min after WIN stimulation	-23.70	-46.61 to -0.7937	Yes	*	0.0406
15 min after WIN stimulation	-19.70	-44.26 to 4.860	No	ns	0.1634
30 min after WIN stimulation	-35.82	-54.95 to -16.69	Yes	***	0.0002
60 min after WIN stimulation	-26.70	-56.97 to 3.577	No	ns	0.1042

C **CB1R_6A-YFP + GRK3-Rluc8 +- SGIP1**

ANOVA table	SS	DF	MS	F (DFn, DFd)	P value
Time x +- SGIP1	752.9	5	150.6	F (5, 80) = 2.776	P=0.0231
Time	3873	5	774.6	F (2.474, 39.58) = 14.28	P<0.0001
+- SGIP1	122.9	1	122.9	F (1, 16) = 1.095	P=0.3108

D **CB1R_8A-YFP + GRK3-Rluc8 +- SGIP1**

ANOVA table	SS	DF	MS	F (DFn, DFd)	P value
Time x +- SGIP1	371.8	5	74.36	F (5, 80) = 1.187	P=0.3231
Time	1134	5	226.8	F (3.327, 53.23) = 3.619	P=0.0157
+- SGIP1	1.071	1	1.071	F (1, 16) = 0.005455	P=0.9420

Table 5. Statistical analysis of kinetics of presented protein-protein interactions. *Curves were compared by two-way ANOVA followed by Sidak's multiple comparison test. If the curves were significantly different, post hoc analysis of time points was performed.*

CB1R-YFP + ß-arrestin2-Rluc – CB1R, CB1R_2A, CB1R_6A, CB1R_8A

ANOVA table	SS	DF	MS	F (DFn, DFd)	P value
Time x CB1R variant	4037	15	269.1	F (15, 160) = 2.709	P=0.0010
Time	6623	5	1325	F (3.664, 117.3) = 13.33	P<0.0001
CB1R variant	6412	3	2137	F (3, 32) = 20.31	P<0.0001

Šídák's multiple comparisons test	Mean Diff.	95.00% CI of diff.	Below threshold?	Summary	Adjusted P Value
0 min					
CB1R vs. CB1R_2A	3.975	-3.738 to 11.69	No	ns	0.4657
CB1R vs. CB1R_6A	2.515	-5.670 to 10.70	No	ns	0.8090
CB1R vs. CB1R_8A	4.040	-2.256 to 10.34	No	ns	0.2753
5 min					
CB1R vs. CB1R_2A	13.41	3.295 to 23.52	Yes	**	0.0099
CB1R vs. CB1R_6A	25.44	16.73 to 34.15	Yes	****	<0.0001
CB1R vs. CB1R_8A	24.66	17.33 to 31.99	Yes	****	<0.0001
10 min					
CB1R vs. CB1R_2A	16.76	3.889 to 29.63	Yes	**	0.0095
CB1R vs. CB1R_6A	26.08	15.65 to 36.50	Yes	****	<0.0001
CB1R vs. CB1R_8A	25.48	13.11 to 37.85	Yes	***	0.0001
15 min					
CB1R vs. CB1R_2A	7.380	-8.523 to 23.28	No	ns	0.5235
CB1R vs. CB1R_6A	15.89	6.848 to 24.93	Yes	***	0.0008
CB1R vs. CB1R_8A	18.19	5.630 to 30.76	Yes	**	0.0049
30 min					
CB1R vs. CB1R_2A	4.511	-15.05 to 24.07	No	ns	0.9066
CB1R vs. CB1R_6A	6.602	-10.88 to 24.08	No	ns	0.6796
CB1R vs. CB1R_8A	10.87	-6.153 to 27.89	No	ns	0.2651
60 min					
CB1R vs. CB1R_2A	0.7437	-16.29 to 17.78	No	ns	0.9992
CB1R vs. CB1R_6A	2.150	-15.91 to 20.21	No	ns	0.9849
CB1R vs. CB1R_8A	-2.384	-20.23 to 15.46	No	ns	0.9788

Table 6. Statistical analysis of kinetics of presented protein-protein interactions. *Curves were compared by two-way ANOVA followed by Sidak's multiple comparison test. If the curves were significantly different, post hoc analysis of time points was performed.*

A **CB1R-YFP + ß-arrestin2-Rluc +- SGIP1**

ANOVA table	SS	DF	MS	F (DFn, DFd)	P value
Time x +- SGIP1	4799	5	959.8	F (5, 95) = 7.702	P<0.0001
Time	32246	5	6449	F (2.222, 42.23) = 51.76	P<0.0001
+- SGIP1	14155	1	14155	F (1, 19) = 90.51	P<0.0001

Šídák's multiple comparisons test	Mean Diff.	95.00% CI of diff.	Below threshold?	Summary	Adjusted P Value
CB1R vs CB1R + SGIP1					
0 min	3.561	-3.424 to 10.55	No	ns	0.5754
5 min after WIN stimulation	-20.24	-26.60 to -13.89	Yes	****	<0.0001
10 min after WIN stimulation	-33.77	-46.43 to -21.10	Yes	****	<0.0001
15 min after WIN stimulation	-29.90	-39.31 to -20.48	Yes	****	<0.0001
30 min after WIN stimulation	-29.97	-50.39 to -9.538	Yes	**	0.0030
60 min after WIN stimulation	-18.19	-42.16 to 5.768	No	ns	0.2082

B **CB1R_2A-YFP + ß-arrestin2-Rluc +- SGIP1**

ANOVA table	SS	DF	MS	F (DFn, DFd)	P value
Time x +- SGIP1	1502	5	300.4	F (5, 80) = 2.566	P=0.0332
Time	10293	5	2059	F (3.343, 53.49) = 17.58	P<0.0001
+- SGIP1	1533	1	1533	F (1, 16) = 7.890	P=0.0126

Šídák's multiple comparisons test	Mean Diff.	95.00% CI of diff.	Below threshold?	Summary	Adjusted P Value
CB1R vs CB1R + SGIP1					
0 min	-3.811	-12.49 to 4.866	No	ns	0.7501
5 min after WIN stimulation	-5.929	-18.19 to 6.332	No	ns	0.6554
10 min after WIN stimulation	-17.69	-30.32 to -5.060	Yes	**	0.0055
15 min after WIN stimulation	-14.55	-33.18 to 4.071	No	ns	0.1720
30 min after WIN stimulation	-8.504	-30.32 to 13.31	No	ns	0.8336
60 min after WIN stimulation	5.272	-15.68 to 26.22	No	ns	0.9702

C **CB1R_6A-YFP + ß-arrestin2-Rluc +- SGIP1**

ANOVA table	SS	DF	MS	F (DFn, DFd)	P value
Time x +- SGIP1	1502	5	300.4	F (5, 80) = 2.566	P=0.0332
Time	10293	5	2059	F (5, 80) = 17.58	P<0.0001
+- SGIP1	1533	1	1533	F (1, 16) = 7.890	P=0.0126

Šídák's multiple comparisons test	Mean Diff.	95.00% CI of diff.	Below threshold?	Summary	Adjusted P Value
CB1R vs CB1R + SGIP1					
0 min	8.039	-0.6709 to 16.75	No	ns	0.0790
5 min after WIN stimulation	-1.879	-15.85 to 12.10	No	ns	0.9991
10 min after WIN stimulation	0.4922	-11.38 to 12.36	No	ns	>0.9999
15 min after WIN stimulation	3.491	-9.635 to 16.62	No	ns	0.9662
30 min after WIN stimulation	1.389	-8.755 to 11.53	No	ns	0.9988
60 min after WIN stimulation	10.08	-8.389 to 28.55	No	ns	0.5371

D **CB1R_8A-YFP + ß-arrestin2-Rluc +- SGIP1**

ANOVA table	SS	DF	MS	F (DFn, DFd)	P value
Time x +- SGIP1	161.3	5	32.27	F (5, 80) = 0.3685	P=0.8687
Time	478.0	5	95.61	F (3.074, 49.18) = 1.092	P=0.3622
+- SGIP1	170.2	1	170.2	F (1, 16) = 1.030	P=0.3253

Table 7. Statistical analysis of kinetics of presented protein-protein interactions. *Curves were compared by two-way ANOVA followed by Sidak's multiple comparison test. If the curves were significantly different, post hoc analysis of time points was performed.*